Catalysts **2015**, *5*, 1574-1602; doi:10.3390/catal5031574

OPEN ACCESS

catalysts

ISSN 2073-4344

www.mdpi.com/journal/catalysts

Review

Nitrogen-Doped Carbon Nanotube and Graphene Materials for Oxygen Reduction Reactions

Qiliang Wei [1,2,†], Xin Tong [2,†], Gaixia Zhang [2], Jinli Qiao [3], Qiaojuan Gong [1,*] and Shuhui Sun [2,*]

[1] Department of Applied Chemistry, Yuncheng University, 1155 Fudan West Street, Yun Cheng 04400, China; E-Mail: qiliang.wei@emt.inrs.ca

[2] Institut National de la Recherche Scientifique (INRS), Centre Énergie, Matériaux et Télécommunications, 1650 Boulevard Lionel-Boulet, Varennes, QC J3X 1S2, Canada; E-Mails: xin.tong@emt.inrs.ca (X.T.); gaixia.zhang@emt.inrs.ca (G.Z.)

[3] College of Environmental Science and Engineering, Donghua University, 2999 Ren'min North Road, Shanghai 201620, China; E-Mail: qiaojl@dhu.edu.cn

† These authors contributed equally to this work.

* Authors to whom correspondence should be addressed; E-Mails: gqjuan@163.com (Q.G.); shuhui@emt.inrs.ca (S.S.); Tel.: +86-0359-8594394 (Q.G.); +1-514-228-6919 (S.S.); Fax: +1-450-929-8102 (S.S.).

Academic Editor: Minhua Shao

Received: 28 May 2015 / Accepted: 1 September 2015 / Published: 14 September 2015

Abstract: Nitrogen-doped carbon materials, including nitrogen-doped carbon nanotubes (NCNTs) and nitrogen-doped graphene (NG), have attracted increasing attention for oxygen reduction reaction (ORR) in metal-air batteries and fuel cell applications, due to their optimal properties including excellent electronic conductivity, $4e^-$ transfer and superb mechanical properties. Here, the recent progress of NCNTs- and NG-based catalysts for ORR is reviewed. Firstly, the general preparation routes of these two N-doped carbon-allotropes are introduced briefly, and then a special emphasis is placed on the developments of both NCNTs and NG as promising metal-free catalysts and/or catalyst support materials for ORR. All these efficient ORR electrocatalysts feature a low cost, high durability and excellent performance, and are thus the key factors in accelerating the widespread commercialization of metal-air battery and fuel cell technologies.

Keywords: nitrogen-doped carbon nanotubes; nitrogen-doped graphene; metal-free catalysts; ORR

1. Introduction

Developing highly efficient electrocatalysts to facilitate sluggish cathodic oxygen reduction reaction (ORR) is a key issue in metal-air batteries and fuel cells [1–5]. The ORR mechanism includes two different pathways: (i) a four-electron ($4e^-$) process to produce water directly though the reaction of oxygen, electrons and protons, and (ii) a two-electron ($2e^-$) process to create the intermediate compound (hydrogen peroxide) [6]. The $4e^-$ process is more attractive for cathode catalysts in fuel cells. Although the platinum-based materials are the better choices for the desired $4e^-$ pathway, the use of very expensive and rare platinum is a major impediment to the development and widespread commercialization of fuel cells. Thus, exploring the substitutes for platinum catalysts by employing non-precious metal catalysts is a very promising direction [7]. In this regard, one-dimensional (1D) carbon nanotubes (CNTs) and two-dimensional (2D) graphene (Figure 1) have attracted a great deal of attention for ORR due to their excellent electronic conductivity, huge specific surface area (SSA), as well as excellent thermal and mechanical properties [8]. Interestingly, when the heteroatoms are incorporated in the carbonaceous skeleton, the ORR performance can be greatly enhanced by effectively modulating the chemisorption energy of O_2, catalytic sites, and the reaction mechanism ($2e^-/4e^-$) of catalysts [9]. Among various possible dopants, N-doped carbon materials are attracting much more attention because of their excellent electrocatalytic performance, low cost, excellent stability, and environmental friendliness, thus setting up a new generation of the metal-free catalysts for ORR. Furthermore, when the nitrogen with excessive valence is introduced to the graphitic plane, more π-electrons can be obtained [10]. This feature, together with the significant difference in the electronegativity of N and C, leads to many unique properties to graphitic carbons, including increased n-type carrier concentration, high surface energy, reduced work-function, as well as tunable polarization [11–14]. As schematically illustrated in Figure 2, three common bonding configurations of N atoms in graphene are demonstrated, including pyrrolic, pyridinic, and graphitic (or quaternary) N [15]. Pyridinic N atoms are located at the edges of graphene planes, and each N atom is bonded to two C atoms and donates one π-electron to the π system. In the case of pyrrolic N atoms, they are incorporated into the heterocyclic rings and each N atom is bonded to two C atoms, contributing two π-electrons to the π system. Graphitic (or quaternary) N refers to the N atoms that replace the carbon atoms in the graphene plane. Such doped N atoms can change the local density state around the Fermi level of N-doped graphitic carbons, which may play a vital role in tailoring the electronic properties and improving their ORR performance [14,16].

On the other hand, metal oxides are also good candidates for ORR catalysts, although they normally suffer from low conductivity, as well as dissolution, sintering, and agglomeration during operation. Consequently, the electrocatalysts show poor electrochemical properties, restricting their applications. NCNTs or NG could effectively buffer the catalyst nanoparticle agglomeration and enhance the electronic conductivity by virtue of their intrinsic excellent conductivity and huge SSA. Therefore,

NCNTs and NG can be used as both excellent metal-free electrocatalysts and perfect catalyst support for ORR.

The basic principles and mechanisms behind N doping effectively tailoring the electrical and surface properties of graphitic carbons have been reviewed in some excellent papers [14,17,18]. Here in this review, we place emphasis on the synthesis of NCNTs and NG, and their applications for ORR.

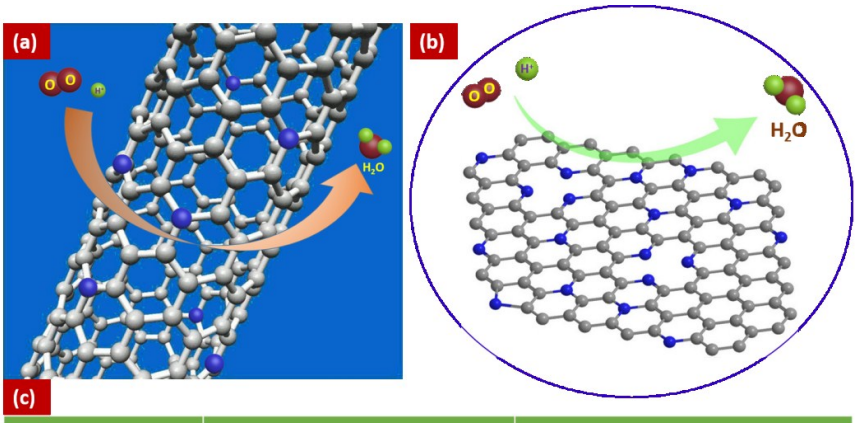

Pathway	Acidic medium	Alkaline medium
$4e^-$	$O_2 + 4H^+ + 4e^- \rightarrow 2H_2O$	$O_2 + 2H_2O + 4e^- \rightarrow 4OH^-$
$2e^-$	$O_2 + 2H^+ + 2e^- \rightarrow H_2O_2$	$O_2 + H_2O + 2e^- \rightarrow HO_2^- + OH^-$
	$H_2O_2 + 2H^+ + 2e^- \rightarrow 2H_2O$	$H_2O + 2HO_2^- + 2e^- \rightarrow 3OH^-$

Figure 1. Illustration of ORR on (**a**) NCNTs; (**b**) NG and (**c**) ORR pathway in acid and alkaline medium. Reproduced and adapted in part from [19]. Copyright © 2013, Rights Managed by Nature Publishing Group.

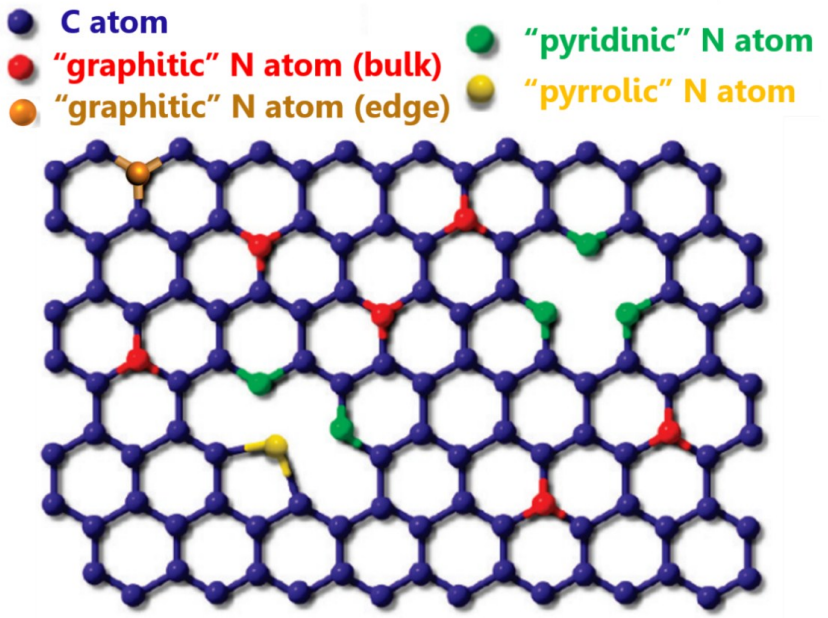

Figure 2. Schematic representation of different types of N atoms (graphitic, pyridinic and pyrrolic N) in NG and NCNTs. Modified with permission from Ref. [20]. Copyright © 2009, American Chemical Society.

2. Synthesis of Nitrogen-Doped Carbon

Nitrogen (N) is a neighboring element of carbon in the periodic table, and its electronegativity (3.04) is larger than that of C (2.55). The incorporation of N atom into a graphene lattice plane could modulate the local electronic properties, as it could form strong bonds with carbon atoms because of its comparable atomic size with carbon. Subsequently, it could generate a delocalized conjugated system between the graphene π-system and the lone pair of electrons from N atom. The introduction of N into carbon nanomaterials could improve both reactivity and electrocatalytic performance. As a result, the N-doped carbon materials have been intensively studied among all the available heteroatoms for doping.

2.1. N-Doped Carbon Nanotubes

NCNTs have become a focus as ORR catalysts due to their high activity and excellent stability. In principle, the N-doping methods can be classified to two categories: *in situ* doping and post-treatment doping [17].

2.1.1. *In Situ* Doping

In situ doping involves the direct incorporation of N heteroatoms into carbon matrix during the preparation process, and it is often used for the preparation of NCNTs. The typical *in situ* doping techniques include high-temperature arc-discharge [21,22], chemical vapor deposition (CVD) [23–27], chemically solvothermal procedures (*ca.* 230–300 °C), [28] and laser ablation methods [29,30]. Thus far, a wide range of N-containing precursors have been used to incorporate N into C matrix with great success. Moreover, the final amount and functionality of N in NCNTs are much more critical for practical applications but could essentially be derived from many different precursors by tuning the synthesis parameters such as temperature of pyrolysis. Among various techniques, CVD is the most promising method to synthesize NCNTs with a different C source (such as methane, acetylene, ethylene, benzene, *etc*.) [31–34] and N source (such as ethylene diamine, dimethylformamide, imidazole, Fe-Phthalocyanine, benzylamine, *etc.*) [34–38]. For instance, recently, by using a co-pyrolysis route of Fe-Phthalocyanine loaded and PEO_{20}-PPO_{70}-PEO_{20} (P123) retained in mesoporous silica, Wang *et al.* [34] synthesized NCNTs with well-defined morphology and graphitic structure, which exhibited good performance for ORR. Based on CVD, She *et al*. fabricated N-doped 1D macroporous carbonaceous nanotube arrays in anodic alumina oxide (AAO) template, which also showed high performance for ORR [27]. In addition to the precursors and pyrolysis temperatures, for each method, other factors, such as time, gas flow rate, catalysts, also have significant influence on the nitrogen contents and the accurately controlled doping sites [17,28,39,40].

2.1.2. Post-Treatment

NCNTs have also been prepared by various post-treatment methods [41,42]. For instance, Nagaiah *et al.* [41] synthesized NCNTs by post-thermal treating oxidized CNTs with ammonia and used the resultant NCNTs as efficient catalysts for ORR in alkaline medium. However, the post-synthesis treatments [43] normally require high temperature (800−1200 °C) and toxic N precursors (NH_3 or

pyridine) which limit their practical application. Moreover, some structural degradation and morphological defects often appear in the materials due to the high temperature treatment [44].

In general, the *in situ* doping tends to form pyrrolic- and/or pyridinic-N atoms, while the graphitic-N in carbon frameworks is normally generated after a high temperature post-treatment [45]. Yet, to obtain an accurate N content and doping sites controllably in these materials is still a challenging problem [17].

2.2. N-Doped Graphene

Compared to doping N into CNTs, the N atom can be more easily introduced into the graphene due to the more open structure in graphene. The N atom could be incorporated into graphene directly during the synthesis of graphene or through post-treatment of graphene oxide (GO) (or graphene). Among numerous methods to produce graphene, CVD, solvothermal fabrication and arc-discharge are normally chosen for *in situ* growth of NG. Compared with the *in situ* synthesis, post-treatment methods which include thermal annealing, plasma or irradiation treatment, or solution treatment are simpler and likely closer to commercialization [46].

2.2.1. *In Situ* Doping

CVD is one of the important methods to prepare NG [20]. In Liu's group, they used Cu/Si as the catalyst, CH_4 as the C source and NH_3 as the N source to produce few-layers NG under 800 °C for the first time (single-layer graphene can be occasionally detected). On the other hand, by using the sole source that contains both C and N (e.g., acetonitrile [47] and pyridine [48]), N atoms can be simultaneously introduced into the graphene lattice during CVD growth of graphene films. The doping amount of N can be adjusted in the range of 1.2–16 at.% by controlling the gas flow rate and the C source to N source ratio [20,49].

A solvothermal process to obtain NG through the reaction between tetrachloromethane and lithium nitride was also developed by Deng *et al.* [50]. It is a one-pot direct synthesis with just placing the reaction reagent in an autoclave and keeping under N_2 and below 350 °C. It allows scalable synthesis and the nitrogen species can be introduced into the graphene structure with 4.5–16.4 at.% of N.

With the presence of pyridine vapor or NH_3, the arc-discharge technique which is commonly used for preparing carbon-based nanomaterials is also employed to fabricate NG. Rao *et al.* [51–53] successfully produced NG with the N content around 0.5–1.5 at.%. However, this process requires complicated purification steps with low yield due to the excessive by-products.

2.2.2. Post-Treatment

Thermal treatment in ammonia atmosphere is an easy and commonly used method to obtain NG by post-modification. Since the N incorporation reactions occur mostly at the defect sites and the edges of graphene, a low N level (e.g., 2.8 at.% in ref.) in graphene is normally obtained in previous reports [54]. In order to get higher N doping, researchers turned their attention to GO which contains a range of reactive oxygen functional groups and more defects to provide more active deposition. In Dai's group [55,56], through thermal annealing of GO under NH_3 atmosphere, the GO nanosheets were

reduced and decorated with N simultaneously. At 300 °C, the N-doping process started, while the highest doping level of ~5 at.% N was achieved at 500 °C. The melamine was also used as the N source to synthesize NG and the atomic percentage of N can reach up to 10.1 at.% [57].

Since the chemical defects in graphene play a critical role in the production of NG, some physically based methods such as plasma treatment or ion implantation are used to induce chemical defects [58]. Furthermore, by changing the plasma density or exposure time, the N content can be easily controlled (up to 8.5 at.% N) [59]. For example, Guo *et al.* used N^+-ion irradiation to introduce defects into the plane of the graphene, and then followed by annealing under NH_3 atmosphere to get NG [60]. The level of N doping can also be adjusted by changing the experimental parameters.

In liquid phase environment, the reduction of GO and N doping can be realized simultaneously under the hydrothermal reaction by using N-containing reducing agent such as hydrazine hydrate [61] or urea [62]. At a pH of 10 and temperature of 80 °C, in the presence of hydrazine and ammonia, slightly wrinkled and folded NG sheets (up to 5 at.% N) were obtained. Also, the N-enriched urea could play a key role in the formation of the NG with high N-doping level (10.13 at.%). During the hydrothermal process, NH_3 will release and react with the oxygen-containing groups on GO; meanwhile, the N atoms can dope into a graphene skeleton. Researchers can control the N-doping level through adjusting the experimental parameters, e.g., the mass ratio between GO and the reducing agent, or the reaction temperature.

3. Nitrogen-Doped Carbon Nanotubes (NCNTs) for Oxygen Reduction Reaction (ORR)

3.1. NCNTs as a Metal-Free Catalyst for ORR

The pioneering work of NCNTs as highly efficient electrocatalysts for ORR in alkaline fuel cells was reported by Gong *et al.* in 2009 [6]. A steady-state output potential of −80 mV and a current density of 4.1 mA/cm^2 at −0.22 V were observed in their study, which is superior to that of −85 mV and 1.1 mA/cm^2 at −0.20 V for a Pt/C electrode. Quantum mechanics calculations show that the carbon atoms adjacent to N dopants have very high positive charge density in order to counterbalance the strong electronic affinity of the N atom. Coupled with aligning the NCNTs, the vertically aligned (VA)-NCNTs show an excellent performance of a $4e^-$ pathway for ORR. Following this important study, plenty of research has been conducted to fabricate NCNTs [37,41,62,63] and to investigate their electrocatalytic activity from both mechanistic and experimental perspectives [23,38,64–68]. For example, based on B3LYP (a trustworthy calculation for nanomaterials) [69–71], Hu *et al.* [69] investigated the adsorption and activation of triplet O_2 on the surface of NCNTs with different diameters and lengths by density functional theory (DFT). The results showed that N doping sufficiently improved the adsorption ability of O_2 on CNTs [69]. Changing the diameter and length of NCNTs has a large effect on the binding energy between O_2 and NCNT and bond length of O_2, and this result further proves that NCNTs are very promising metal-free catalysts for ORR from a theoretical perspective.

From an experimental perspective, in 2009, Y. Tang *et al.* [72] synthesized NCNTs via the CVD method using acetonitrile or ethanol as precursors and Ar/H_2 as carrier gases. TEM images indicate that the NCNTs are composed of individual nanocups stacked together (Figure 3). Their results

indicated that the stacked NCNTs exhibited similar catalytic activity with Pt/CNTs in ORR and they can also be used in the electrochemical detection of H_2O_2 and glucose. Using the CVD method, several other research groups also tried to synthesize NCNTs with different N precursors. Experiments indicate that carbon and N precursors have a significant impact on the morphology and performance of NCNTs. For instance, when ferrocene (catalyst precursor) and imidazole (C and N precursor) were used, the as-synthesized NCNTs had a high N content of 8.54 at.% and a bamboo-like structure [23]; by annealing CNTs and tripyrrolyl[1,3,5]triazine (TPT) mixture in N, the NCNTs annealing at 900 °C exhibited excellent electrochemical performance towards ORR in alkaline medium [73].

In another group, Kundu *et al.* fabricated NCNTs via the pyrolysis of acetonitrile with cobalt as catalyst at different temperatures in order to control the nitrogen content [63]. The results indicated that NCNTs prepared at lower temperatures had a higher amount of pyridinic groups with more exposed edge planes. Furthermore, they proved that the NCNTs with a higher amount of pyridinic groups possess better catalytic properties for ORR. Later, they synthesized NCNTs using a new approach, *i.e.*, by treating oxidized CNTs with ammonia at 800 °C; the obtained NCNTs exhibited a favorable positive onset potential for ORR, increased reduction current, and excellent stability, demonstrating a very promising cathode catalyst for ORR in alkaline medium [41]. Almost at the same time, Chen and co-workers synthesized NCNTs using various N precursors and/or catalysts [74–77]. It was concluded from their studies that higher N content and more defects in NCNTs lead to higher ORR performance. Similar conclusions were also drawn by Geng *et al.* [78]. However, others have found that there is no direct correlation between total N content and the ORR performance; for example, a recent study reported, through post-treatment of few-walled carbon nanotubes (FWCNTs) with polyaniline, a much lower N content (~0.5 at.%). Interestingly, the low N-containing FWCNTs exhibited excellent electrocatalytic activity for ORR as well as higher methanol tolerance properties [79]. Therefore, the exact role of N doping in NCNTs for the ORR activity is still under debate. Until recently, Wågberg *et al.* [45] investigated how a thermal post-treatment on the N-doped MWCNTs can result in the transformation of pyrrolic and pyridinic N sites into quaternary N sites (N-Q_s), leading to the improvement of ORR performance. They reached the conclusion that the quaternary N valley sites (N-Q_{valley}) are the most active sites in NCNTs for ORR; hence, a $4e^-$ reduction pathway occurs generally on the N edge defects. Based on this fundamental concept, the chemical functionalization becomes an alternative and effective approach to introducing N into complex carbon nanostructures [80]. Accordingly, Tuci *et al.* reported a systematic study on the synthesis, characterization, and electrocatalytic property of MWCNTs functionalized with a series of well-defined pyridine groups [81]. They also discussed the role of the electronic charge density distribution at the chemically grafted N heterocycles on the ORR performance. This study therein introduced a deep level of complexity to the understanding of the ultimate role of the pyridine groups on ORR in NCNTs.

All these findings introduced above have significant impacts on catalysis and fuel cell domains. However, most of the CNTs used in these reports were synthesized by the pyrolysis of a nitrogen-containing precursor, and the residual catalyst particles of Fe or Co were removed by the electrochemical method. Though great attention has been paid to the purification process, the effects of metal contaminates in NCNTs on the ORR performance are still controversial, unless NCNTs could be obtained by a metal-free synthetic process. In this regard, by employing water-plasma etching SiO_2/Si wafers, Dai's group reported a simple but effective approach for the growth of densely packed

N-doped single-walled CNTs [82]. Figure 4a shows the schematic illustration of the NCNT fabrication process. Typically, the water-plasma was used to etch the SiO_2 coating (30 nm) on the top of the SiO_2/Si wafer to produce uniform SiO_2 nanoparticles, which will act as the catalysts for NCNT growth during the CVD synthesis. As shown in Figure 4b–e, the produced metal-free NCNTs showed superb electrocatalytic activity and excellent durability toward ORR in acidic medium. For the similar purpose of excluding the possible contribution of metal impurities to ORR catalysis, Wang *et al.* [64] discovered that, without metal-containing catalysts, N atoms alone show strong promotion for the self-assembly of NCNTs from gaseous carbons. Based on this new discovery, pure metal-free CNTs with a high level of N doping (20 at.%) can be directly synthesized by using melamine as both the carbon and nitrogen precursor, without any post-treatment. More importantly, such intact samples can be used to investigate the intrinsic catalytic activity of NCNTs more clearly; the results indicated that NCNTs indeed performed very well. Furthermore, Li *et al.* reported that the concentration of KOH electrolyte also had a large impact on the ORR performance of the NCNTs [65]. Higher concentration of KOH electrolyte leads to more negative onset potential and lower current densities. For example, when the concentration of KOH increased from 0.1 M to 12 M, the diffusion-limiting current decreased over 100 times. This could be attributed to the very low oxygen solubility in highly concentrated KOH electrolytes. In addition, in 3 M and 6 M KOH electrolytes, NCNTs showed competitive activity with commercial Pt/C catalyst for ORR in alkaline media, and much better activity than the Ag/C catalyst [65].

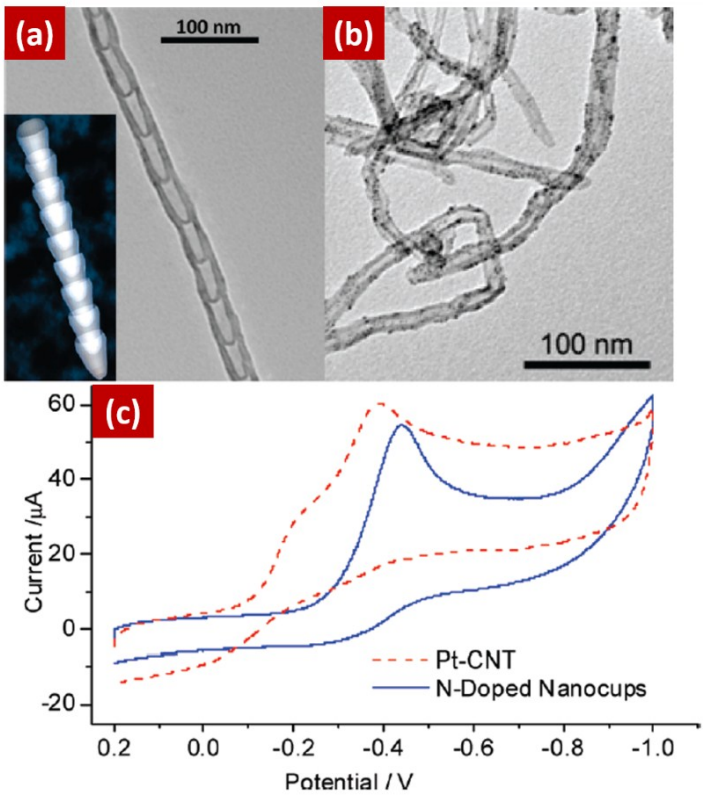

Figure 3. (**a**,**b**) TEM image of stacked NCNTs and commercial Pt-CNTs. Inset in (**a**) is the scheme illustration of the nanocups in stacked NCNTs. (**c**) CV curves of stacked NCNTs and commercial Pt-CNTs in 0.1 M KOH aqueous solution saturated with O_2. Reprinted with permission from Ref. [72] Copyright © 2009, American Chemical Society.

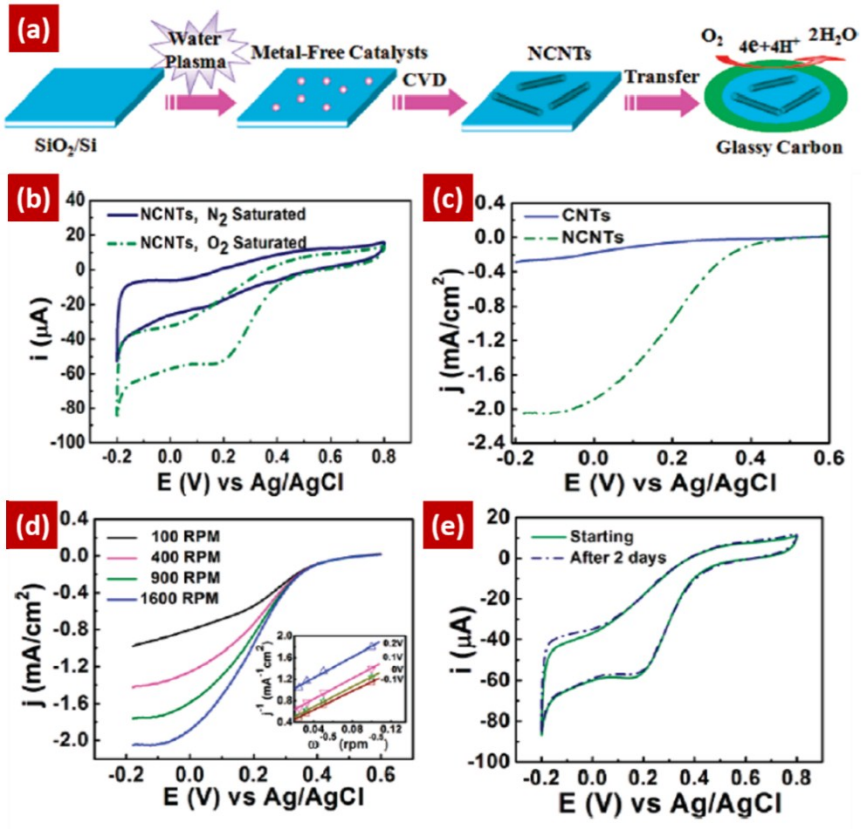

Figure 4. (**a**) Water-plasma-assisted CVD growth of NCNTs for the ORR; (**b**) CVs of the NCNTs, 50 mV/s in 0.5 M H_2SO_4 solution saturated with N_2 or O_2; (**c**) RDE curves of the NCNTs and CNTs in oxygen-saturated 0.5 M H_2SO_4; (**d**) RDE curves of the NCNT in oxygen-saturated 0.5 M H_2SO_4, inset: Koutecky-Levich plots of the NCNT derived from RDE measurements; (**e**) The two-day stability measurements of the NCNT by using continuous CV in oxygen-saturated 0.5 M H_2SO_4. Reprinted with permission from [82]. Copyright © 2010, American Chemical Society.

3.2. NCNTs as Catalyst Support Material for ORR

Using CNTs as catalyst supports have attracted significant interest because of their high surface area and excellent electrical conductivity. The N doping creates defects on the surface of pristine CNTs and breaks out its chemical inertness, while preserving its electrical conductivity [83]; moreover, NCNTs contain nitrogenized sites that are electrochemically active. Therefore, NCNTs were also used as excellent supports for catalyst nanoparticles. For instance, Vijayaraghavan *et al.* demonstrated that Pt nanoparticles/NCNTs exhibited enhanced catalytic activity and stability along with N-dopant contents [84]. Later, Sun's group demonstrated that uniform Pt nanoparticles with smaller size and better ORR activity than pure CNTs were obtained from NCNTs [85,86] (Figure 5). The authors also demonstrated that the catalyst stability increased with the increase of N contents in NCNTs [87]. To further take the merits of both carbon and ceramic-based supports for ORR, the Sun group employed the composite nanostructures of NCNTs coated with $TiSi_2O_x$ as Pt catalyst supports, and the results indicated that this composite showed better ORR performance than Pt/NCNT catalysts, thereby illustrating its promise as a catalyst for fuel cells [88]. Chen's group concluded that the

NCNTs synthesized from an N-rich precursor solution (ethylenediamine) exhibited superior catalytic activity toward ORR compared with NCNTs grown from a precursor solution with relatively low N content pyridine [89].

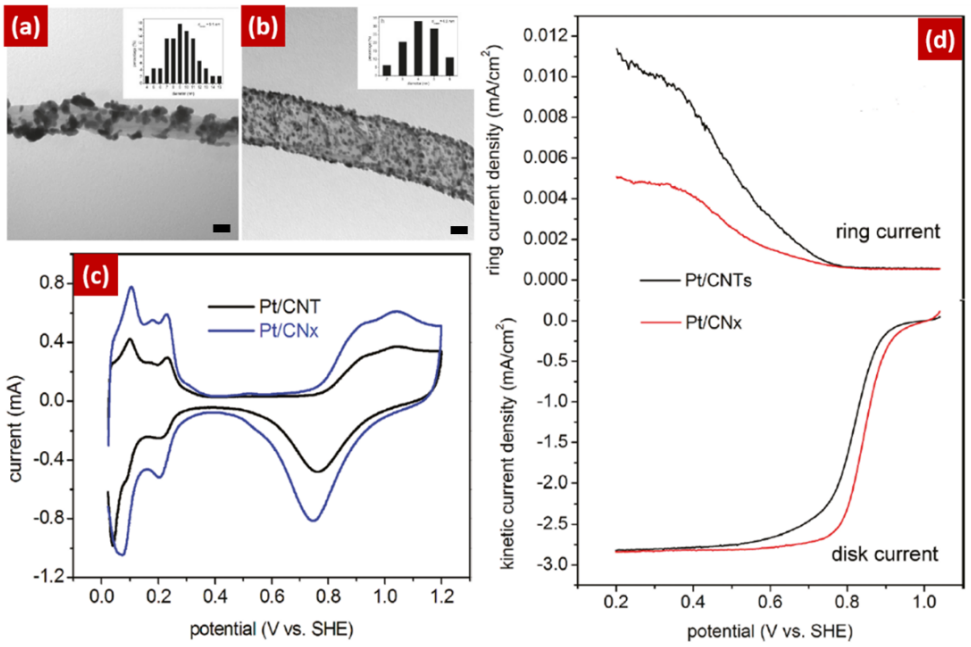

Figure 5. (**a**,**b**) TEM images and size distribution of Pt/CNTs (**a**) and Pt/CN_x (**b**) (scale bars are 20 nm); (**c**) CVs of Pt/CNTs an Pt/CNx 0.5 M H_2SO_4 with saturated Ar at 50 mV/s; (**d**) RRDE results of Pt/CNTs and Pt/CN_x in 0.5 M H_2SO_4 saturated with O_2 at 5 mV/s at the rotation speed of 1600 rpm at room temperature. Reprinted with permission from [85]. Copyright © 2011, American Chemical Society.

4. Nitrogen-Doped Graphene (NG) for ORR

As discussed above, NCNTs could act as efficient and effective metal-free catalysts for ORR. Carbon atoms adjacent to nitrogen dopants could create a net positive charge density in order to counterbalance the strong electronic affinity of the N atom [6]. Hence the doping of the N atom could readily attract electrons to facilitate the ORR. Similar to NCNTs, coupled with the recent popularity of graphene, NG is also considered an appealing candidate for the applications in ORR where the NCNTs have already been exploited significantly.

4.1. NG as a Metal-Free Catalyst for ORR

Compared with NCNTs, NG has a large surface area and outstanding electrical conductivity; moreover, it also has the unique graphitic basal plane structure that could further facilitate electron transport and supply more active sites.

In 2010, Qu *et al.* first reported the application of NG as catalysts for the ORR [90]. As shown in Figure 6, a free-standing NG film of 4 cm^2 in size consisting of only a few layer sheets was obtained by the CVD method, using gas mixtures of NH_3, CH_4, H_2 and Ar on the Ni catalyst surface. The N content in the as-synthesized NG was *ca.* 4 at.%. The RRDE voltammograms measurements were

conducted, in alkaline electrolyte, to investigate the catalytic properties of NG, graphene and Pt/C for ORR. From Figure 6b, it can be seen that the graphene electrode showed a 2 e^- process for ORR with an onset potential of around −0.45 V. After doping with N, the NG electrode exhibited a one-step, 4 e^- pathway for ORR.

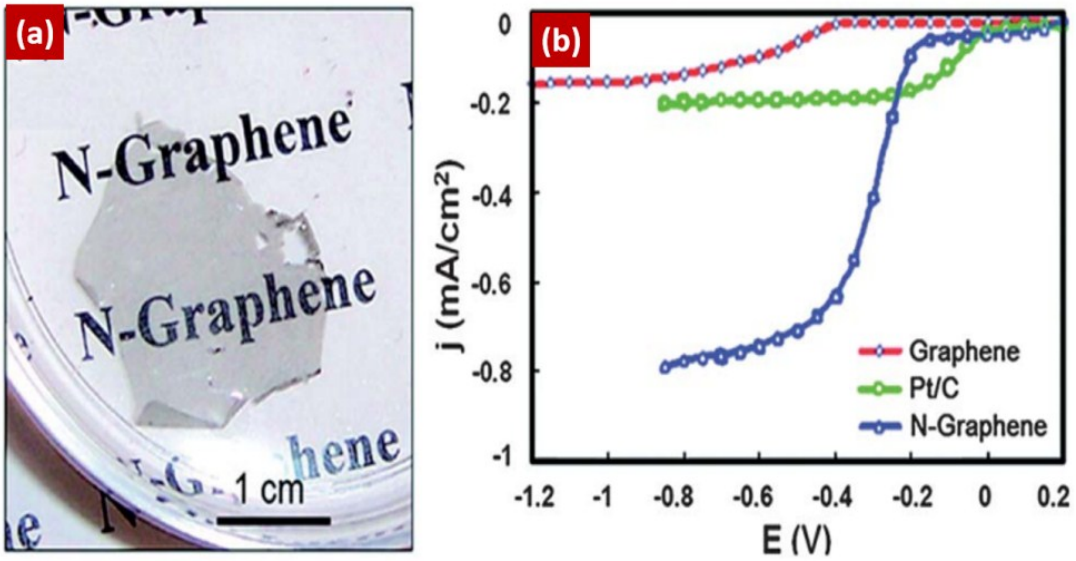

Figure 6. (**a**) An optical photograph of NG film floating on water; (**b**) LV curves in 0.1 M KOH saturated with air of different samples. Reprinted with permission from [90]. Copyright © 2010, American Chemical Society.

Calculated by the Koutecky-Levich equation, the transferred electron number per O_2 molecule of the NG was 3.6–4. It was found that the steady-state catalytic current density of the NG electrode was three times higher than the commercial Pt/C electrode. Similar to NCNTs, NG has excellent durability and good selectivity for ORR. The accelerated degradation test (ADT), which was carried out by CV in O_2-saturated electrolyte, is used to estimate the stability of the catalyst. In previous work, the graphene showed obviously more stable catalytic performance than Pt/C. Almost no significant loss in the voltammetric charge was observed after even a 100,000-cycle stability test [91]. Another advantage of NG compared to Pt for ORR is that ORR on NG is not greatly affected by methanol [59,90] and CO [90,92]. For instance, a 40% decrease was observed at the Pt/C electrode on the introduction of 2% (*w*/*w*) methanol [90], whereas the NG electrode remained unaffected under the identical condition. The high selectivity of NG toward ORR makes it very attractive for implementation in different kinds of fuel cells.

Based on these results, numerous research studies have been conducted on NG for ORR. Some of the typical works are summarized in Table 1. It is notable that the half-wave potential and onset potential for ORR are important criteria for evaluating the activity of an electrocatalyst, and the number of the electron transfer is determined from RRDE measurements to show that whether the electron transfer mechanism is a 2e^- dominated process or 4e^- dominated process.

Table 1. Summary of some typical work dedicated to NG as a metal-free catalyst for ORR.

Synthesis Method and Reactants	N-Content (at.%)	Electrocatalytic Performance	Electron Transfer Number	Ref.
Thermal treatment of glucose and urea	33	NG (25 at.%) shows competitive ORR activities with Pt/C and much better crossover resistance and excellent stability	3.2–3.7	[19]
CVD (C source, ethylene; N source, ammonia; Cu)	up to16	Higher onset potential as compared to Pt/C	close to 2	[49]
Thermal treatment of GO using melamine	10.1	Much higher ORR activity than grapheme	3.4–3.6	[57]
N plasma treatment on graphene	8.5	Higher ORR activity than graphene, and higher durability and selectivity than Pt/C	-	[59]
CVD (C source, methane; N source, ammonia, Cu)	4	Higher activity, better stability and tolerance to crossover than Pt	3.6–4	[90]
Detonation technique with cyanuric chloride and trinitrophenol	12.5	Comparable to that of Pt, more stable and less expensive	3.69	[91]
A resin-based methodology with N-containing resin and metal ions	1.8	The onset potential on the NG electrode is close to that of Pt/C. The current is almost the same for both the Pt/C and NG	2.1–3.9	[92]
Hydrothermal reaction of GO with urea	6.05–7.65	The performance of these NG materials towards ORR is still not as good as that of Pt/C in terms of the half-wave potential and current density	~3	[93]
Covalent functionalize GO using organic molecules and thermal treatment	0.72–4.3	The NG nanosheet exhibited a good electrocatalytic activity through an efficient one-step, $4e^-$ pathway	3.63	[94]
CVD of N-containing aromatic precursor molecules	2.0–2.7	The N dopants in the graphene reduce the ORR overpotential, thereby enhancing the catalytic activity	3.5–4.0	[95]
GO treatment by ammonia hydroxide, heating under ammonia gas, and reaction with melamine	6.0–6.8	Pyridinic N plays a vital role in ORR	3.2–3.7	[96]
Annealing of GO with ammonia and N-containing polymers	2.91–7.56	The higher limiting current density compared to Pt	2.85–3.65	[97]
Thermal reaction between GO and NH_3	2.4–4.6	The onset potential is close to that of Pt/C	~3.8	[98]
Hydrothermal reaction with GO and melamine	26.08	It shows lower ORR activity than Pt/C 40 wt.%	3.2–4.0	[99]
Hydrothermal process using urea and holey GO	8.6	Superb ORR with $4e^-$ pathway and excellent durability	3.85	[100]
Thermally annealing GO with melamine	8.05	The nG-900 exhibits lower activity and onset potential than Pt/C, albeit higher than graphene; excellent stability	3.3–3.7	[101]

Table 1. *Cont.*

Synthesis Method and Reactants	N-content (at.%)	Electrocatalytic Performance	Electron Transfer Number	Ref.
Pyrolyzing GO with urea	7.86	The NG showed a much-higher activity than glassy carbon (GC) and graphene	3.6–4.0	[102]
Redox GO with pyrrole then thermal treatment	6	Shows comparable onset potentials with 40 wt.% Pt/C	3.3	[103]
GO and dicyandiamide under hydrothermal condition	7.78	The onset potentials at rGO-N was lower than that at Pt/C	2.6	[104]
Pyrolysis of graphene oxide and polyaniline	2.4	High activity toward ORR with a superior long-term stability and tolerance to methanol crossover	3.8–3.9	[105]
Thermally annealing GO 5-aminotetrazole monohydrate	10.6	Higher current density than Pt/C. Lower onset potential of ORR than that of the commercial Pt/C	3.7	[106]
Pyrolysis of sugar in the presence of urea	3.02–11.2	The NG1000 has comparable ORR half-wave potential to 20 wt.% Pt/C	3.2–3.8	[107]
Hydrothermal reaction of GO with urea	5.8–6.2	NG has higher ORR activity than grapheme, but is not yet comparable to the Pt	3.0–4.0	[108]
Pyrolysis of GO and polydopamine	2.78–3.79	Much more enhanced ORR activities with positive onset potential and larger current density than graphene	3.89	[109]
Pyrolyzing GO with Melamine, urea and dicyandiamide	5	Compared to Pt/C, the half-wave potential of ORR on this NG catalyst was close, wheras the n values are slightly lower	3.5–4	[110]
PANI acting as a N source were deposited on the surface of GNRs via a layer-by-layer approach	4.1–8.3	Very good electrocatalytic activity and stability	3.91	[111]
NG is synthesized by pyrolyzing ion exchange with resin and glycine	0.98–1.65	Doping N in graphene is good to improve the activity for ORR, but still lower than Pt/C catalyst	-	[112]
Microwave heating of graphene under NH_3 flow	4.05–5.47	The doping of graphite N enhanced the activity of the catalysts in the ORR in alkaline solution	3.03–3.3	[113]
Facile hydrothermal method	2.8	Competitive with the commercial Pt/C catalysts in alkaline medium	3.66–3.92	[114]
Gas-phase oxidation strategy using a nitric acid vapor	0.52	The onset potential is (0.755 V *vs.* RHE), comparable to the value of chemically synthesized NG, and the current densities are higher than those demonstrated for NG.	3.2–3.9	[115]
CVD growth of graphene and post-doping with a solid N precursor of graphitic C_3N_4	6.5	Excellent activity, high stability, and very good crossover resistance for ORR in alkaline medium.	3.96-4.05	[116]
A hard templating approach	5.07	Outstanding ORR performance in both acidic and alkaline solutions.	3.9	[117]

In spite of extensive studies, the explanations on the exact catalytic mechanisms of NG (e.g., wherein the N configuration (pyridinic N or graphitic N) is more important for the ORR activity) or even the active sites are still controversial [94,118]. In Sun *et al.*'s research [55], they found that NG containing 0.3892% quaternary N (the highest N content in three samples) showed the best ORR activity and the relationship between ORR activity and graphitic N contents matched very well. It revealed that graphitic type N plays the vital role for ORR activity. Luo *et al.* [49] synthesized the graphene layers doped with nearly 100% pyridinic N through the pyrolysis of methane (CH_4) and NH_3 on Cu substrate, and the as-synthesized pyridinic N-doped graphene mainly exhibited a $2e^-$ transfer process for ORR, indicating that pyridinic N may not, as previously expected, effectively promote the $4e^-$ ORR performance of carbon materials.

On the contrary, in the work of Sheng [57], the NG mainly containing pyridine-like N atoms was obtained by the heat-treatment of GO in the presence of melamine. Since the electrocatalytic activity of the NGs toward ORR is independent of N-doping level, it may indicate that the pyridine-like N in NGs determines its ORR activity. Pyridinic N, which has a lone electron pair in the plane of the carbon matrix, could donate the electron to the π-bond, attract electrons, and therefore be catalytically active. Some results were shown in many previous works [94–96].

In the research of Ruoff's group [97], NG with different N-doping formats was prepared by annealing GO together with different N-containing precursors, such as ammonia and N-containing polymers. It was prone to generate graphitic N and pyridinic N when annealing GO with ammonia, while it tended to form pyridinic and pyrrolic N species when annealing GO with polyaniline or polypyrrole. They found that the total atomic content of N rarely affects the ORR activity under alkaline conditions. Actually, the graphitic N-dominated catalysts exhibit higher catalytic activity and larger limiting current density than that of pyrrolic or pyridinic N-dominated catalysts. However, the pyridinic N could enhance the ORR onset potential and gradually convert the $2e^-$ dominated pass-way to the $4e^-$ dominated process. Also, some researchers [119–122] used the periodic DFT to simulate the ORR at the edge of NG. For example, by taking into account the experimental conditions, *i.e.*, the surface coverage, the water effect, the bias effect and pH, Yu *et al.* [119] presented a systematic theoretical study on the full reaction path of ORR on NG. They concluded that the rate-determining step is the O(ads) removal from the NG surface. From another perspective, by calculating energy variations during each reaction step using DFT, Zhang and Xia [120] demonstrated that the electrocatalytic activity of NG is related to the atomic charge density distribution and electron spin density The reasons for why NG has catalytic capability (while pristine graphene does not) have also been discussed. From Kim *et al.*'s results, [121] doping of N in graphene could promote the oxygen adsorption, the first electron transfer, and the selectivity toward the $4e^-$ reduction pathway. More specifically, they suggested that the outermost graphitic N sites are the main active sites. Meanwhile, they also proposed that the graphitic N site which involves a ring-opening of the cyclic C-N bond at the edge of graphene could result in the pyridinic N, thus, the inter-converts conversion mechanism between pyridinic and graphitic types during the catalytic cycle may reconcile the experimental controversy about what types of N are the ORR active sites for N-doped carbon materials [121].

Besides the doped N species, the morphology of NG also plays a significant role for the ORR properties. During the doping process of graphene, the stacking of graphene sheets is inclined to increase the diffusion resistance of reactants/electrolytes, reduce the specific area, and the exposed

active sites. It is thus worth controlling the structure of NG to get more ORR activity. In this regard, there is a great deal of work on the production of N-doped holey graphene [99,100]. For instance, a 3D porous nanostructure which has N-doped holes on individual graphene sheets was synthesized through a hydrothermal process using urea and holey GO by Yu *et al.* [100]. Benefiting from the 3D porous nanostructure, abundant exposed sites, and high-level N doping, the as-prepared material exhibited excellent ORR performance, such as the high limiting current, strong resistance to the methanol crossover, which are competitive with the commercial 20 wt.% Pt/C catalysts.

4.2. NG as Support Material for ORR

The incorporation of N atoms within graphene sheets could contribute more functional groups, higher electron-mobility, and more active sites for catalytic reactions. Also, it is beneficial for facilitating the distribution and uniformity of metal nanoparticles. Moreover, when NG acts as the support, it could enhance the catalytic properties due to the interaction between graphene and metal nanoparticles. Consequently, NG materials have been regarded as one very promising metal catalyst support [123–126].

Typically, NG is proposed to be able to stabilize the noble metal nanoparticles, and improve the durability of the catalysts. Moreover, nitrogen doping could introduce active sites for catalytic reactions and also act as anchoring sites for metal nanoparticle deposition. Yang *et al.* fabricated a composite of Pt-Au alloy nanoparticles on NG sheets by a wet-chemistry method [127]. As shown in Figure 7, the NG was synthesized by thermal treatment of GO powder and melamine. Then the solutions of H_2PtCl_6, $HAuCl_4$, NG in DMF and water underwent the microwave irradiation. The as-prepared Pt_3Au-NPs were found to be well dispersed on the NG sheets (Figure 7b) and the HRTEM image in Figure 7c revealed the lattice fringes of the NPs have an interplanar spacing of 0.232 nm. The fast Fourier transforms (FFTs) shown in Figure 7d indicated the single crystallite nature of the Pt_3Au/NG on (111) plane. Figure 7e,f showed that the corresponding potential for Pt_3Au/NG was much lower than the other two samples at a given oxidation current density. Improved electrocatalytict activity was observed due to the small size, uniform dispersion and a high electrochemical active surface area of the nanocomposites. Recently, more studies on NG- or N-rGO-supported Pt electrocatalysts have also been reported; all these results demonstrate the significant function of N doping in producing highly efficient ORR electrocatalysts [128–130].

Additionally, it was predicted that non-precious-metal-NG hybrid materials would also lead to enhanced catalytic properties. For instance, Chen *et al.* reported a strategy to synthesize ZnSe/NG nanocomposites (NG-ZnSe) [131]. As shown in Figure 8, $[ZnSe](DETA)_{0.5}$ nanobelts were gradually put into the GO solution, and then the sediments were processed by hydrothermal treatment. As shown in Figure 8b, ZnSe nanorods, which were composed of ZnSe nanoparticles, were grown on a graphene surface. It can be seen from Figure 8c that the NG-ZnSe electrode exhibited higher positive onset potential and larger current for ORR. The improved performance can be attributed to the synergetic effects between NG and alloy nanostructures. There are also a number of similar reports using non-precious metal to produce metal/NG composites, showing potential applications [132–136].

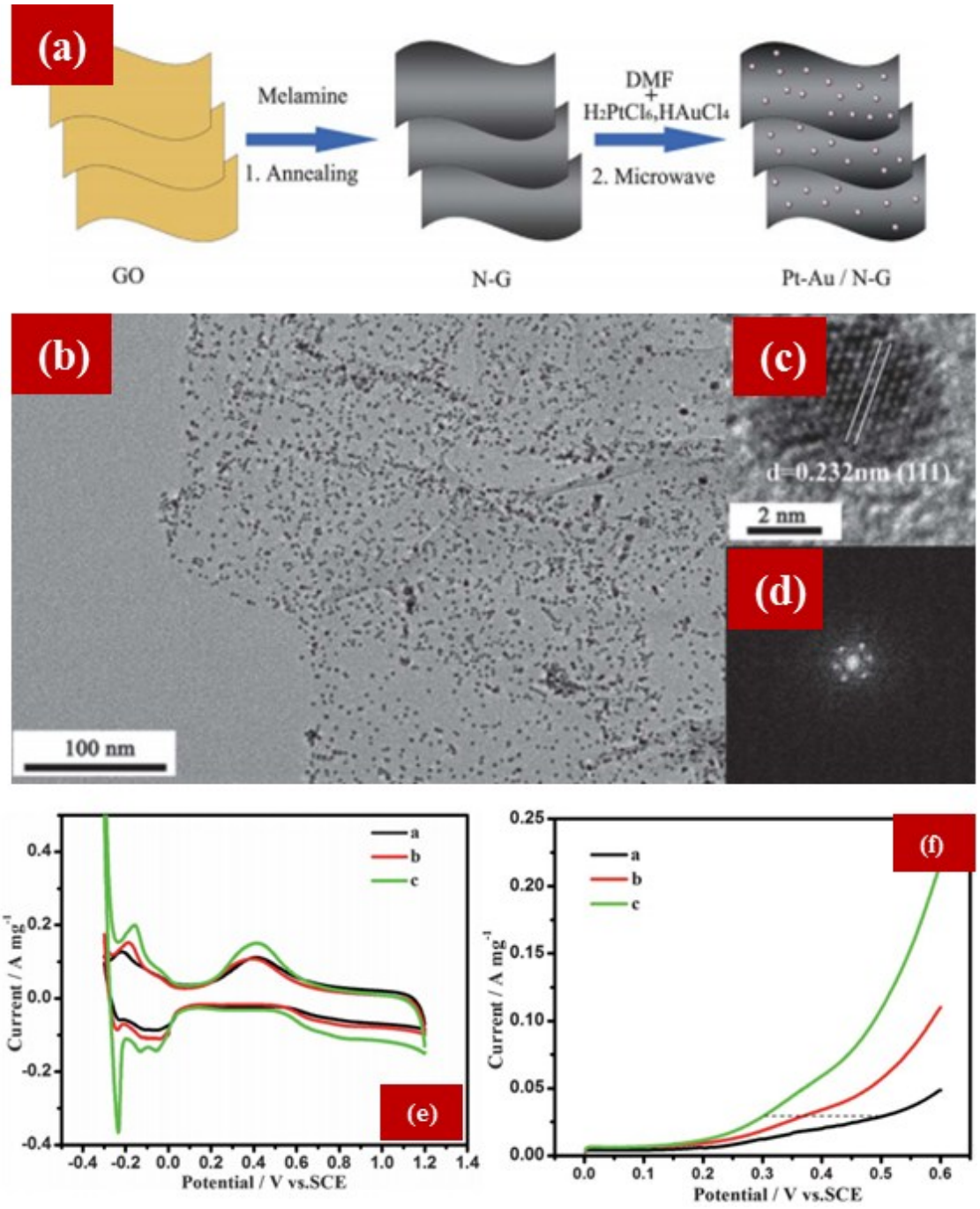

Figure 7. (**a**) Fabrication of the Pt-Au alloy NPs on the NG sheets; (**b**) TEM of Pt_3Au/N-G; (**c**) HRTEM and (**d**) FFTs of a single Pt_3Au NP on NG; (**e**) CVs and (**f**) LSV of Pt/C (a, black), Pt_3Au/G(b, red) and Pt_3Au/N-G catalysts (c, green). Reprinted with permission from [127]. Copyright © 2012, Royal Society of Chemistry.

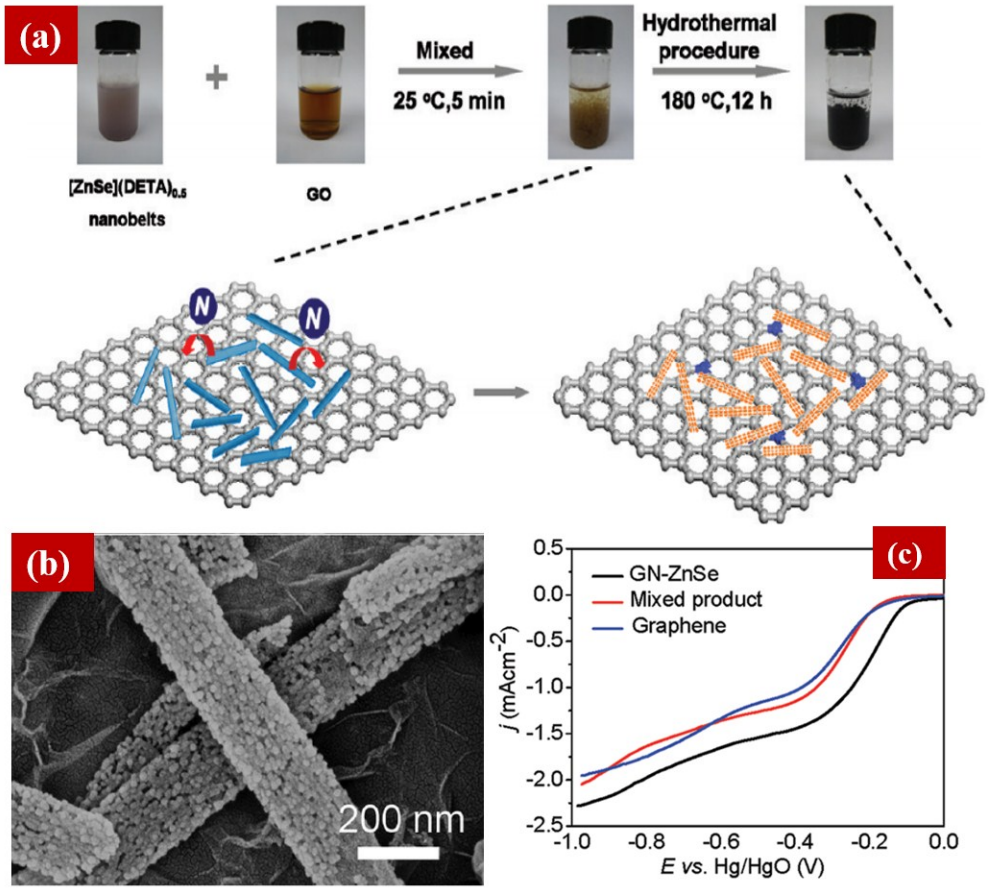

Figure 8. (**a**) Schematic preparation of NG-ZnSe nanocomposites (blue rods-$[ZnSe](DETA)_{0.5}$ nanobelts; orange rods-ZnSe nanorods; purple balls-N; gray balls-C); (**b**) SEM photograph of ZnSe/NG; (**c**) LV curves in 1.0 M KOH solution with saturated O_2 of different electrodes. Reprinted with permission from Ref. [131]. Copyright © 2012, American Chemical Society. Note: in the original paper, the authors refer to "nitrogen-doped graphene" as "GN"; here in this review, for consistency, we named it "NG."

5. The Composites of NCNTs and NG for ORR

As a two-dimensional layer structure of sp^2-hybridized carbon, graphene has strong direction-dependent transport properties and is easily agglomerated and restacked to graphite; therefore, when used as a catalyst, it may result in declined activity. A combination of CNT and graphene may be an effective way to solve this problem [137,138]. Dai's group has demonstrated that CNT-graphene complexes can exhibit excellent activity and stability towards ORR in both acidic and basic electrolytes [139]. Furthermore, based on the STEM-HAADF and EELS mapping results, they speculated that the impurities of nitrogen and iron might be the reason for the excellent ORR properties. While, as illustrated in the previous sections, NCNTs and NG have shown excellent electrocatalytic performance for the ORR compared with pure CNTs or graphene. Therefore, , there have recently been efforts to hybridize these two carbon structures (NCNTs and NG) to obtain a synergy effect to further improve their catalytic performance [138,140]. For example, Ma *et al.* fabricated the 3D NCNTs/graphene composite through the pyrolysis of pyridine over the Ni catalyst supported on graphene sheet [140]. The N content in the NCNTs/NG composite was about 6.6 at.%, compared with the undoped CNTs/G;

the doped sample showed higher catalytic activity and selectivity for ORR in the alkaline electrolyte. Another example of highly active N-doped G/CNT composite electrocatalyst for ORR is demonstrated by Ratso and coworkers [141]. N-doped few-layer G/CNT composite was fabricated by the pyrolysis of GO/MWCNT with urea and dicyandiamide. Based on the XPS and RDE results, they concluded that the enhanced electrocatalytic activity is due to a higher content of pyridinic N in the samples, and the higher limiting currents of oxygen reduction can be ascribed by the quaternary N. These results are attractive for alkaline fuel cells. However, these methods require high temperature pyrolysis, during which the morphological defects and structural degradation are probably shown up in the final products [17]. In this regard, Chen *et al.* synthesized NG-NCNT nanocomposite through a hydrothermal process at a much lower temperature (*i.e.*, 180 °C) (Figure 9a) [44]. The diameters of the nanotubes are in the range of 9−15 nm, and the atomic percentages of N content are 3.2 at.% and 1.3 at.% for graphene and CNTs, respectively, which confirm the existence of the N element in both graphene and CNTs. This NG-NCNT displayed a $4e^-$ pathway for ORR with more positive onset potential, large peak current, and good durability (Figure 9b–g). Very recently, however, a hybrid of NCNT and graphene prepared by plasma-enhanced CVD showed inferior ORR activity, [142] which is contradictory to the above-mentioned results. The reason for this discrepancy is still not clear, thus extensive and careful research in this area is still needed.

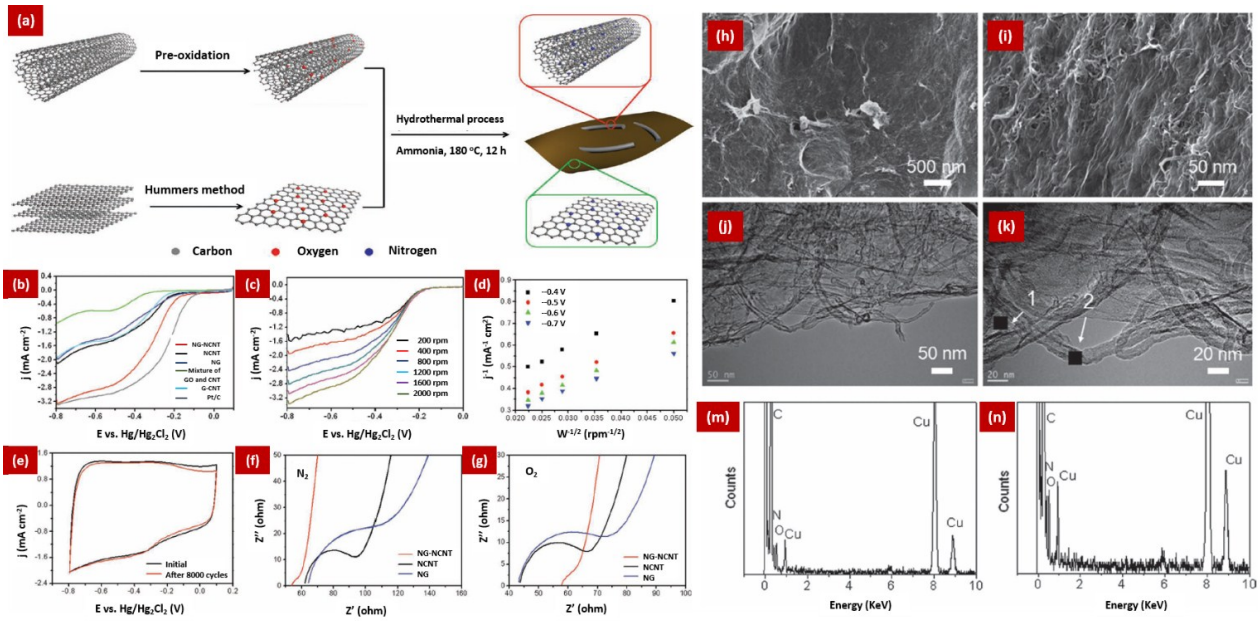

Figure 9. (**a**) Schematic preparation of the NG-NCNT nanocomposites; (**b**) LV curves in 0.1 M KOH solution with the rotation speed of 1600 rpm and sweep rate of 20 $mV \cdot s^{-1}$in oxygen of different samples; (**c**) LV curves of NG-NCNT with different rotation speeds (sweep rate 20 $mV \cdot s^{-1}$); (**d**) K-L plots (i^{-1} *vs.* $\omega^{-1/2}$) at different potentials (*vs.* Hg/Hg_2Cl_2); (**e**) CVs of GN-CNT after 8000 cycles with the sweep rate of 150 $mV \cdot s^{-1}$; (**f**–**g**) Impedance data of different samples in 0.1 M KOH solution with saturated N_2 and O_2, respectively; (**h**–**k**) SEM and STEM images of the typical NG-NCNT nanocomposite; (**m**,**n**) Elemental analysis image of the NG and NG-NCNT (the area marked with 1 and 2 in Figure (**k**) respectively. Reprinted with permission from [44]. Copyright © 2013 WILEY-VCH Verlag GmbH & Co. KGaA, Weinheim.

6. Conclusion and Perspectives

ORR plays an essential role in energy-related areas, such as metal-air batteries and fuel cells, and traditionally, the Pt-based catalysts are regarded as the best choice for $4e^-$ ORR. Due to the prohibitive price and scarcity of Pt, the development of high performance and inexpensive metal-free and non-noble metal catalysts, to replace Pt, are highly desired, and it plays an important role in promoting the large-scale practical applications of these energy devices. Due to their outstanding properties, such as ultrahigh charge carrier mobility, gigantic thermal conductivity, extremely large surface area, exceptional mechanical strength and flexibility, CNTs and graphene have been extensively explored for ORR. The pristine CNTs and graphene mainly exhibit $2e^-$ pathway for ORR, while N doping has been proved to be a promising way to tailor their properties to promote $4e^-$ ORR which is much more meaningful for energy applications. For N doping in CNTs or graphene, there are mainly two strategies: the first method is the *in situ* doping where nitrogen can be doped into CNTs or graphene nanosheets during the growing process with the addition of proper carbon and nitrogen sources. The second one is the post-treatment process; in this method, CNTs or GO were firstly synthesized, then annealed at high temperatures together with the nitrogen-containing precursors. Despite much progress, it is still not easy to precisely control the N-doping sites and concentration. All of these characteristics affect the ORR properties of NCNTs and NG in the catalytic applications. Therefore, the development of new and more controllable doping methods is still highly desired. Through N doping, various properties, including the surface energy, work function, carrier concentration, and surface polarization, of CNTs and graphene could be tuned, so that NCNTs and NG have become the most promising metal-free catalysts toward $4e^-$ ORR. In general, three common bonding configurations, including graphitic, pyridinic, and pyrrolic N, are normally achieved when doping nitrogen into CNTs and graphene. Different doping strategies would significantly affect the N-doping levels and N types in NCNTs and NG. For example, the *in situ* doping normally generates pyridinic- and/or pyrrolic-N species, while the post-treatment doping is prone to form graphitic-N in carbon frameworks.

In the applications for ORR, from both theoretical and experimental perspectives, researchers have demonstrated that NCNTs and NG show remarkable electrocatalytic performance. In a theoretical context, through DFT simulations, it was shown that in NCNTs and NG, the carbon atoms with higher spin density usually possess more active sites. Through investigating the reaction mechanisms, it was proved that the removal of $O_{(ads)}$ on the surface of nitrogen-doped carbon determines the reaction rate. In the experimental part, the developments of both NCNTs and NG as metal-free ORR catalysts and as the metal catalyst support for ORR are summarized in detail in this review. All the N-doped carbon materials (NCNTs, NG) exhibit higher catalytic performance compared to their pristine counterparts (CNTs, graphene), indicating a great beneficial effect of N doping on the ORR performance. Moreover, the progresses on NCNTs- and NG-based composites for ORR have also been discussed in this review, demonstrating that it is also a very promising research direction for next-generation non-noble metal or metal-free ORR catalysts. Although much progress has been achieved in the area of NCNTs and NG for ORR catalysts, challenges still exist: (i) New and greener methods are required for the large-scale production of NCNTs and NG; (ii) The control of N doping at specific positions in CNTs and graphene is still lacking; (iii) A careful controlling of nitrogen sites, types and concentration is still highly desired; (iv) The deep understanding of oxygen adsorption and reduction on these

NCNTs- and NG-based catalysts is still lacking, and therefore, systematic theoretical simulations are also needed, which may boost the developments of N-doping carbon materials for ORR in the future.

Acknowledgments

We thank the support from Natural Science Foundations of China, the Natural Science Foundation of Shanxi Province, Fonds de Recherche du Québec-Natureet Technologies (FRQNT), the Natural Sciences and Engineering Research Council of Canada (NSERC), Institut National de la Recherche Scientifique (INRS), and Centre Québécois sur les MateriauxFonctionnels (CQMF) and China Scholarship Council (CSC).

Author Contributions

Qiliang Wei was the leading author from the initial draft writing to the finalization of the manuscript. Qiliang Wei and Xin Tong wrote the first draft of the manuscript. All authors contributed as a team to the manuscript plan, revisions, the literature reading, and the proof reading.

Conflicts of Interest

The authors declare no conflict of interest.

References

1. Dai, L.; Xue, Y.; Qu, L.; Choi, H.-J.; Baek, J.-B. Metal-free catalysts for oxygen reduction reaction. *Chem. Rev.* **2015**, *115*, 4823–4892.
2. Cheng, F.; Chen, J. Metal-air batteries: From oxygen reduction electrochemistry to cathode catalysts. *Chem. Soc. Rev.* **2012**, *41*, 2172–2192.
3. Wang, D.-W.; Su, D. Heterogeneous nanocarbon materials for oxygen reduction reaction. *Energy Environ. Sci.* **2014**, *7*, 576–591.
4. Feng, L.; Yan, Y.; Chen, Y.; Wang, L. Nitrogen-doped carbon nanotubes as efficient and durable metal-free cathodic catalysts for oxygen reduction in microbial fuel cells. *Energy Environ. Sci.* **2011**, *4*, 1892–1899.
5. Suntivich, J.; Gasteiger, H.A.; Yabuuchi, N.; Nakanishi, H.; Goodenough, J.B.; Shao-Horn, Y. Design principles for oxygen-reduction activity on perovskite oxide catalysts for fuel cells and metal–air batteries. *Nat. Chem.* **2011**, *3*, 546–550.
6. Gong, K.; Du, F.; Xia, Z.; Durstock, M.; Dai, L. Nitrogen-doped carbon nanotube arrays with high electrocatalytic activity for oxygen reduction. *Science* **2009**, *323*, 760–764.
7. Wei, W.; Liang, H.; Parvez, K.; Zhuang, X.; Feng, X.; Müllen, K. Nitrogen-doped carbon nanosheets with size-defined mesopores as highly efficient metal-free catalyst for the oxygen reduction reaction. *Angew. Chem.* **2014**, *126*, 1596–1600.
8. Sun, D.M.; Liu, C.; Ren, W.C.; Cheng, H.M. A review of carbon nanotube-and graphene-based flexible thin-film transistors. *Small* **2013**, *9*, 1188–1205.
9. Yu, D.; Nagelli, E.; Du, F.; Dai, L. Metal-free carbon nanomaterials become more active than metal catalysts and last longer. *J. Phys. Chem. Lett.* **2010**, *1*, 2165–2173.

10. Chun, K.-Y.; Lee, H.S.; Lee, C.J. Nitrogen doping effects on the structure behavior and the field emission performance of double-walled carbon nanotubes. *Carbon* **2009**, *47*, 169–177.
11. Bostwick, A.; Speck, F.; Seyller, T.; Horn, K.; Polini, M.; Asgari, R.; MacDonald, A.H.; Rotenberg, E. Observation of plasmarons in quasi-freestanding doped graphene. *Science* **2010**, *328*, 999–1002.
12. Hwang, J.O.; Park, J.S.; Choi, D.S.; Kim, J.Y.; Lee, S.H.; Lee, K.E.; Kim, Y.-H.; Song, M.H.; Yoo, S.; Kim, S.O. Work function-tunable, N-doped reduced graphene transparent electrodes for high-performance polymer light-emitting diodes. *ACS Nano* **2011**, *6*, 159–167.
13. Czerw, R.; Terrones, M.; Charlier, J.-C.; Blase, X.; Foley, B.; Kamalakaran, R.; Grobert, N.; Terrones, H.; Tekleab, D.; Ajayan, P. Identification of electron donor states in N-doped carbon nanotubes. *Nano Lett.* **2001**, *1*, 457–460.
14. Lee, W.J.; Maiti, U.N.; Lee, J.M.; Lim, J.; Han, T.H.; Kim, S.O. Nitrogen-doped carbon nanotubes and graphene composite structures for energy and catalytic applications. *Chem. Commun.* **2014**, *50*, 6818–6830.
15. Liu, H.; Liu, Y.; Zhu, D. Chemical doping of graphene. *J. Mater. Chem.* **2011**, *21*, 3335–3345.
16. Yang, Z.; Nie, H.; Chen, X.A.; Chen, X.; Huang, S. Recent progress in doped carbon nanomaterials as effective cathode catalysts for fuel cell oxygen reduction reaction. *J. Power Sources* **2013**, *236*, 238–249.
17. Zheng, Y.; Jiao, Y.; Jaroniec, M.; Jin, Y.; Qiao, S.Z. Nanostructured metal-free electrochemical catalysts for highly efficient oxygen reduction. *Small* **2012**, *8*, 3550–3566.
18. Vazquez-Arenas, J.; Higgins, D.; Chen, Z.; Fowler, M.; Chen, Z. Mechanistic analysis of highly active nitrogen-doped carbon nanotubes for the oxygen reduction reaction. *J. Power Sources* **2012**, *205*, 215–221.
19. Zhang, Y.W.; Ge, J.; Wang, L.; Wang, D.H.; Ding, F.; Tao, X.M.; Chen, W. Manageable N-doped graphene for high performance oxygen reduction reaction. *Sci. Rep.* **2013**, *3*, doi:10.1038/srep02771.
20. Wei, D.; Liu, Y.; Wang, Y.; Zhang, H.; Huang, L.; Yu, G. Synthesis of N-doped graphene by chemical vapor deposition and its electrical properties. *Nano Lett.* **2009**, *9*, 1752–1758.
21. Jung, S.H.; Kim, M.R.; Jeong, S.H.; Kim, S.U.; Lee, O.J.; Lee, K.H.; Suh, J.H.; Park, C.K. High-yield synthesis of multi-walled carbon nanotubes by arc discharge in liquid nitrogen. *Appl. Phys. A* **2003**, *76*, 285–286.
22. Sun, L.; Wang, C.; Zhou, Y.; Zhang, X.; Cai, B.; Qiu, J. Flowing nitrogen assisted-arc discharge synthesis of nitrogen-doped single-walled carbon nanohorns. *Appl. Surf. Sci.* **2013**, *277*, 88–93.
23. Mo, Z.; Liao, S.; Zheng, Y.; Fu, Z. Preparation of nitrogen-doped carbon nanotube arrays and their catalysis towards cathodic oxygen reduction in acidic and alkaline media. *Carbon* **2012**, *50*, 2620–2627.
24. Sharifi, T.; Nitze, F.; Barzegar, H.R.; Tai, C.-W.; Mazurkiewicz, M.; Malolepszy, A.; Stobinski, L.; Wågberg, T. Nitrogen doped multi walled carbon nanotubes produced by CVD-correlating xps and raman spectroscopy for the study of nitrogen inclusion. *Carbon* **2012**, *50*, 3535–3541.
25. Guo, Q.; Zhao, D.; Liu, S.; Chen, S.; Hanif, M.; Hou, H. Free-standing nitrogen-doped carbon nanotubes at electrospun carbon nanofibers composite as an efficient electrocatalyst for oxygen reduction. *Electrochim. Acta* **2014**, *138*, 318–324.

26. Tao, X.Y.; Zhang, X.B.; Sun, F.Y.; Cheng, J.P.; Liu, F.; Luo, Z.Q. Large-scale CVD synthesis of nitrogen-doped multi-walled carbon nanotubes with controllable nitrogen content on a $Co_xMg_{1-x}MoO_4$ catalyst. *Diamond Relat. Mater.* **2007**, *16*, 425–430.
27. She, X.; Yang, D.; Jing, D.; Yuan, F.; Yang, W.; Guo, L.; Che, Y. Nitrogen-doped one-dimensional (1D) macroporous carbonaceous nanotube arrays and their application in electrocatalytic oxygen reduction reactions. *Nanoscale* **2014**, *6*, 11057–11061.
28. Chen, L.; Xia, K.; Huang, L.; Li, L.; Pei, L.; Fei, S. Facile synthesis and hydrogen storage application of nitrogen-doped carbon nanotubes with bamboo-like structure. *Int. J. Hydrogen Energy* **2013**, *38*, 3297–3303.
29. Shi, W.; Venkatachalam, K.; Gavalas, V.; Qian, D.; Andrews, R.; Bachas, L.G.; Chopra, N. The role of plasma treatment on electrochemical capacitance of undoped and nitrogen doped carbon nanotubes. *Nanomater. Energy* **2013**, *2*, 71–81.
30. Du, Z.; Wang, S.; Kong, C.; Deng, Q.; Wang, G.; Liang, C.; Tang, H. Microwave plasma synthesized nitrogen-doped carbon nanotubes for oxygen reduction. *J. Solid State Electrochem.* **2015**, *19*, 1541–1549.
31. Magrez, A.; Seo, J.W.; Smajda, R.; Mionić, M.; Forró, L. Catalytic CVD synthesis of carbon nanotubes: Towards high yield and low temperature growth. *Materials* **2010**, *3*, 4871–4891.
32. Donato, M.G.; Galvagno, S.; Lanza, M.; Messina, G.; Milone, C.; Piperopoulos, E.; Pistone, A.; Santangelo, S. Influence of carbon source and Fe-catalyst support on the growth of multi-walled carbon nanotubes. *J. Nanosci. Nanotechnol.* **2009**, *9*, 3815–3823.
33. Li, J.; Papadopoulos, C.; Xu, J.M.; Moskovits, M. Highly-ordered carbon nanotube arrays for electronics applications. *Appl. Phys. Lett.* **1999**, *75*, 367–369.
34. Wang, Y.; Cui, X.; Li, Y.; Chen, L.; Chen, H.; Zhang, L.; Shi, J. A co-pyrolysis route to synthesize nitrogen doped multiwall carbon nanotubes for oxygen reduction reaction. *Carbon* **2014**, *68*, 232–239.
35. Ayala, P.; Grüneis, A.; Gemming, T.; Grimm, D.; Kramberger, C.; Rümmeli, M.H.; Freire, F.L.; Kuzmany, H.; Pfeiffer, R.; Barreiro, A. Tailoring N-doped single and double wall carbon nanotubes from a nondiluted carbon/nitrogen feedstock. *J. Phys. Chem. C* **2007**, *111*, 2879–2884.
36. Tang, C.; Golberg, D.; Bando, Y.; Xu, F.; Liu, B. Synthesis and field emission of carbon nanotubular fibers doped with high nitrogen content. *Chem. Commun.* **2003**, 3050–3051.
37. Rao, C.V.; Cabrera, C.R.; Ishikawa, Y. In search of the active site in nitrogen-doped carbon nanotube electrodes for the oxygen reduction reaction. *J. Phys. Chem. Lett.* **2010**, *1*, 2622–2627.
38. Rao, C.V.; Ishikawa, Y. Activity, selectivity, and anion-exchange membrane fuel cell performance of virtually metal-free nitrogen-doped carbon nanotube electrodes for oxygen reduction reaction. *J. Phys. Chem. C* **2012**, *116*, 4340–4346.
39. Guo, Q.; Xie, Y.; Wang, X.; Zhang, S.; Hou, T.; Lv, S. Synthesis of carbon nitride nanotubes with the C_3N_4 stoichiometry via a benzene-thermal process at low temperatures. *Chem. Commun.* **2004**, 26–27.
40. Cao, C.; Huang, F.; Cao, C.; Li, J.; Zhu, H. Synthesis of carbon nitride nanotubes via a catalytic-assembly solvothermal route. *Chem. Mater.* **2004**, *16*, 5213–5215.

41. Nagaiah, T.C.; Kundu, S.; Bron, M.; Muhler, M.; Schuhmann, W. Nitrogen-doped carbon nanotubes as a cathode catalyst for the oxygen reduction reaction in alkaline medium. *Electrochem. Commun.* **2010**, *12*, 338–341.
42. Chan, L.H.; Hong, K.H.; Xiao, D.Q.; Lin, T.C.; Lai, S.H.; Hsieh, W.J.; Shih, H.C. Resolution of the binding configuration in nitrogen-doped carbon nanotubes. *Phys. Rev. B* **2004**, *70*, 125408.
43. Vikkisk, M.; Kruusenberg, I.; Ratso, S.; Joost, U.; Shulga, E.; Kink, I.; Rauwel, P.; Tammeveski, K. Enhanced electrocatalytic activity of nitrogen-doped multi-walled carbon nanotubes towards the oxygen reduction reaction in alkaline media. *RSC Adv.* **2015**, *5*, 59495–59505.
44. Chen, P.; Xiao, T.Y.; Qian, Y.H.; Li, S.S.; Yu, S.H. A nitrogen-doped graphene/carbon nanotube nanocomposite with synergistically enhanced electrochemical activity. *Adv. Mater.* **2013**, *25*, 3192–3196.
45. Sharifi, T.; Hu, G.; Jia, X.; Wågberg, T. Formation of active sites for oxygen reduction reactions by transformation of nitrogen functionalities in nitrogen-doped carbon nanotubes. *ACS Nano* **2012**, *6*, 8904–8912.
46. Wood, K.N.; O'Hayre, R.; Pylypenko, S. Recent progress on nitrogen/carbon structures designed for use in energy and sustainability applications. *Energy Environ. Sci.* **2014**, *7*, 1212–1249.
47. Reddy, A.L.M.; Srivastava, A.; Gowda, S.R.; Gullapalli, H.; Dubey, M.; Ajayan, P.M. Synthesis of nitrogen-doped graphene films for lithium battery application. *ACS Nano* **2010**, *4*, 6337–6342.
48. Jin, Z.; Yao, J.; Kittrell, C.; Tour, J.M. Large-scale growth and characterizations of nitrogen-doped monolayer graphene sheets. *ACS Nano* **2011**, *5*, 4112–4117.
49. Luo, Z.; Lim, S.; Tian, Z.; Shang, J.; Lai, L.; MacDonald, B.; Fu, C.; Shen, Z.; Yu, T.; Lin, J. Pyridinic N doped graphene: Synthesis, electronic structure, and electrocatalytic property. *J. Mater. Chem.* **2011**, *21*, 8038–8044.
50. Deng, D.; Pan, X.; Yu, L.; Cui, Y.; Jiang, Y.; Qi, J.; Li, W.-X.; Fu, Q.; Ma, X.; Xue, Q.; *et al.* Toward N-doped graphene via solvothermal synthesis. *Chem. Mater.* **2011**, *23*, 1188–1193.
51. Ghosh, A.; Late, D.J.; Panchakarla, L.S.; Govindaraj, A.; Rao, C.N.R. NO_2 and humidity sensing characteristics of few-layer graphenes. *J. Exp. Nanosci.* **2009**, *4*, 313–322.
52. Panchakarla, L.S.; Subrahmanyam, K.S.; Saha, S.K.; Govindaraj, A.; Krishnamurthy, H.R.; Waghmare, U.V.; Rao, C.N.R. Synthesis, structure, and properties of boron-and nitrogen-doped graphene. *Adv. Mater.* **2009**, *21*, 4726–4730.
53. Subrahmanyam, K.S.; Panchakarla, L.S.; Govindaraj, A.; Rao, C.N.R. Simple method of preparing graphene flakes by an arc-discharge method. *J. Phys. Chem. C* **2009**, *113*, 4257–4259.
54. Geng, D.; Chen, Y.; Chen, Y.; Li, Y.; Li, R.; Sun, X.; Ye, S.; Knights, S. High oxygen-reduction activity and durability of nitrogen-doped graphene. *Energy Environ. Sci.* **2011**, *4*, 760–764.
55. Wang, X.; Li, X.; Zhang, L.; Yoon, Y.; Weber, P.K.; Wang, H.; Guo, J.; Dai, H. N-doping of graphene through electrothermal reactions with ammonia. *Science* **2009**, *324*, 768–771.
56. Li, X.; Wang, H.; Robinson, J.T.; Sanchez, H.; Diankov, G.; Dai, H. Simultaneous nitrogen doping and reduction of graphene oxide. *J. Am. Chem. Soc.* **2009**, *131*, 15939–15944.
57. Sheng, Z.-H.; Shao, L.; Chen, J.-J.; Bao, W.-J.; Wang, F.-B.; Xia, X.-H. Catalyst-free synthesis of nitrogen-doped graphene via thermal annealing graphite oxide with melamine and its excellent electrocatalysis. *ACS Nano* **2011**, *5*, 4350–4358.

58. Wang, H.; Maiyalagan, T.; Wang, X. Review on recent progress in nitrogen-doped graphene: Synthesis, characterization, and its potential applications. *ACS Catal.* **2012**, *2*, 781–794.
59. Shao, Y.; Zhang, S.; Engelhard, M.H.; Li, G.; Shao, G.; Wang, Y.; Liu, J.; Aksay, I.A.; Lin, Y. Nitrogen-doped graphene and its electrochemical applications. *J. Mater. Chem.* **2010**, *20*, 7491–7496.
60. Guo, B.; Liu, Q.; Chen, E.; Zhu, H.; Fang, L.; Gong, J.R. Controllable N-doping of graphene. *Nano Lett.* **2010**, *10*, 4975–4980.
61. Long, D.; Li, W.; Ling, L.; Miyawaki, J.; Mochida, I.; Yoon, S.-H. Preparation of nitrogen-doped graphene sheets by a combined chemical and hydrothermal reduction of graphene oxide. *Langmuir* **2010**, *26*, 16096–16102.
62. Sun, L.; Wang, L.; Tian, C.; Tan, T.; Xie, Y.; Shi, K.; Li, M.; Fu, H. Nitrogen-doped graphene with high nitrogen level via a one-step hydrothermal reaction of graphene oxide with urea for superior capacitive energy storage. *RSC Adv.* **2012**, *2*, 4498–4506.
63. Kundu, S.; Nagaiah, T.C.; Xia, W.; Wang, Y.; Dommele, S.V.; Bitter, J.H.; Santa, M.; Grundmeier, G.; Bron, M.; Schuhmann, W. Electrocatalytic activity and stability of nitrogen-containing carbon nanotubes in the oxygen reduction reaction. *J. Phys. Chem. C* **2009**, *113*, 14302–14310.
64. Wang, Z.; Jia, R.; Zheng, J.; Zhao, J.; Li, L.; Song, J.; Zhu, Z. Nitrogen-promoted self-assembly of N-doped carbon nanotubes and their intrinsic catalysis for oxygen reduction in fuel cells. *ACS Nano* **2011**, *5*, 1677–1684.
65. Li, H.; Liu, H.; Jong, Z.; Qu, W.; Geng, D.; Sun, X.; Wang, H. Nitrogen-doped carbon nanotubes with high activity for oxygen reduction in alkaline media. *Int. J. Hydrogen Energy* **2011**, *36*, 2258–2265.
66. Qiu, Y.; Yin, J.; Hou, H.; Yu, J.; Zuo, X. Preparation of nitrogen-doped carbon submicrotubes by coaxial electrospinning and their electrocatalytic activity for oxygen reduction reaction in acid media. *Electrochim. Acta* **2013**, *96*, 225–229.
67. Wiggins-Camacho, J.D.; Stevenson, K.J. Mechanistic discussion of the oxygen reduction reaction at nitrogen-doped carbon nanotubes. *J. Phys. Chem. C* **2011**, *115*, 20002–20010.
68. Okamoto, Y. First-principles molecular dynamics simulation of O_2 reduction on nitrogen-doped carbon. *Appl. Surf. Sci.* **2009**, *256*, 335–341.
69. Hu, X.; Wu, Y.; Li, H.; Zhang, Z. Adsorption and activation of O_2 on nitrogen-doped carbon nanotubes. *J. Phys. Chem. C* **2010**, *114*, 9603–9607.
70. Barone, V.; Peralta, J.E.; Wert, M.; Heyd, J.; Scuseria, G.E. Density functional theory study of optical transitions in semiconducting single-walled carbon nanotubes. *Nano Lett.* **2005**, *5*, 1621–1624.
71. Nikawa, H.; Yamada, T.; Cao, B.; Mizorogi, N.; Slanina, Z.; Tsuchiya, T.; Akasaka, T.; Yoza, K.; Nagase, S. Missing metallofullerene with C80 cage. *J. Am. Chem. Soc.* **2009**, *131*, 10950–10954.
72. Tang, Y.; Allen, B.L.; Kauffman, D.R.; Star, A. Electrocatalytic activity of nitrogen-doped carbon nanotube cups. *J. Am. Chem. Soc.* **2009**, *131*, 13200–13201.
73. Yang, M.; Yang, D.; Chen, H.; Gao, Y.; Li, H. Nitrogen-doped carbon nanotubes as catalysts for the oxygen reduction reaction in alkaline medium. *J. Power Sources* **2015**, *279*, 28–35.

74. Chen, Z.; Higgins, D.; Tao, H.; Hsu, R.S.; Chen, Z. Highly active nitrogen-doped carbon nanotubes for oxygen reduction reaction in fuel cell applications. *J. Phys. Chem. C* **2009**, *113*, 21008–21013.
75. Chen, Z.; Higgins, D.; Chen, Z. Nitrogen doped carbon nanotubes and their impact on the oxygen reduction reaction in fuel cells. *Carbon* **2010**, *48*, 3057–3065.
76. Higgins, D.; Chen, Z.; Chen, Z. Nitrogen doped carbon nanotubes synthesized from aliphatic diamines for oxygen reduction reaction. *Electrochim. Acta* **2011**, *56*, 1570–1575.
77. Chen, Z.; Higgins, D.; Chen, Z. Electrocatalytic activity of nitrogen doped carbon nanotubes with different morphologies for oxygen reduction reaction. *Electrochim. Acta* **2010**, *55*, 4799–4804.
78. Geng, D.; Liu, H.; Chen, Y.; Li, R.; Sun, X.; Ye, S.; Knights, S. Non-noble metal oxygen reduction electrocatalysts based on carbon nanotubes with controlled nitrogen contents. *J. Power Sources* **2011**, *196*, 1795–1801.
79. Borghei, M.; Kanninen, P.; Lundahl, M.; Susi, T.; Sainio, J.; Anoshkin, I.; Nasibulin, A.; Kallio, T.; Tammeveski, K.; Kauppinen, E. High oxygen reduction activity of few-walled carbon nanotubes with low nitrogen content. *Appl. Catal. B* **2014**, *158*, 233–241.
80. Tuci, G.; Zafferoni, C.; D'Ambrosio, P.; Caporali, S.; Ceppatelli, M.; Rossin, A.; Tsoufis, T.; Innocenti, M.; Giambastiani, G. Tailoring carbon nanotube N-dopants while designing metal-free electrocatalysts for the oxygen reduction reaction in alkaline medium. *ACS Catal.* **2013**, *3*, 2108–2111.
81. Tuci, G.; Zafferoni, C.; Rossin, A.; Milella, A.; Luconi, L.; Innocenti, M.; Truong Phuoc, L.; Duong-Viet, C.; Pham-Huu, C.; Giambastiani, G. Chemically functionalized carbon nanotubes with pyridine groups as easily tunable N-decorated nanomaterials for the oxygen reduction reaction in alkaline medium. *Chem. Mater.* **2014**, *26*, 3460–3470.
82. Yu, D.; Zhang, Q.; Dai, L. Highly efficient metal-free growth of nitrogen-doped single-walled carbon nanotubes on plasma-etched substrates for oxygen reduction. *J. Am. Chem. Soc.* **2010**, *132*, 15127–15129.
83. Sun, S.; Zhang, G.; Zhong, Y.; Liu, H.; Li, R.; Zhou, X.; Sun, X. Ultrathin single crystal Pt nanowires grown on N-doped carbon nanotubes. *Chem. Commun.* **2009**, 7048–7050.
84. Vijayaraghavan, G.; Stevenson, K.J. Synergistic assembly of dendrimer-templated platinum catalysts on nitrogen-doped carbon nanotube electrodes for oxygen reduction. *Langmuir* **2007**, *23*, 5279–5282.
85. Chen, Y.; Wang, J.; Liu, H.; Banis, M.N.; Li, R.; Sun, X.; Sham, T.-K.; Ye, S.; Knights, S. Nitrogen doping effects on carbon nanotubes and the origin of the enhanced electrocatalytic activity of supported Pt for proton-exchange membrane fuel cells. *J. Phys. Chem. C* **2011**, *115*, 3769–3776.
86. Saha, M.S.; Li, R.; Sun, X.; Ye, S. 3-d composite electrodes for high performance pem fuel cells composed of Pt supported on nitrogen-doped carbon nanotubes grown on carbon paper. *Electrochem. Commun.* **2009**, *11*, 438–441.
87. Chen, Y.; Wang, J.; Liu, H.; Li, R.; Sun, X.; Ye, S.; Knights, S. Enhanced stability of Pt electrocatalysts by nitrogen doping in CNTs for PEM fuel cells. *Electrochem. Commun.* **2009**, *11*, 2071–2076.

88. Banis, M.N.; Sun, S.; Meng, X.; Zhang, Y.; Wang, Z.; Li, R.; Cai, M.; Sham, T.-K.; Sun, X. $TiSi_2O_x$ coated N-doped carbon nanotubes as Pt catalyst support for the oxygen reduction reaction in PEMFCs. *J. Phys. Chem. C* **2013**, *117*, 15457–15467.
89. Higgins, D.C.; Meza, D.; Chen, Z. Nitrogen-doped carbon nanotubes as platinum catalyst supports for oxygen reduction reaction in proton exchange membrane fuel cells. *J. Phys. Chem. C* **2010**, *114*, 21982–21988.
90. Qu, L.; Liu, Y.; Baek, J.-B.; Dai, L. Nitrogen-doped graphene as efficient metal-free electrocatalyst for oxygen reduction in fuel cells. *ACS Nano* **2010**, *4*, 1321–1326.
91. Feng, L.Y.; Chen, Y.G.; Chen, L. Easy-to-operate and low-temperature synthesis of gram-scale nitrogen-doped graphene and its application as cathode catalyst in microbial fuel cells. *ACS Nano* **2011**, *5*, 9611–9618.
92. He, C.Y.; Li, Z.S.; Cai, M.L.; Cai, M.; Wang, J.Q.; Tian, Z.Q.; Zhang, X.; Shen, P.K. A strategy for mass production of self-assembled nitrogen-doped graphene as catalytic materials. *J. Mater. Chem. A* **2013**, *1*, 1401–1406.
93. Wu, J.J.; Zhang, D.; Wang, Y.; Hou, B.R. Electrocatalytic activity of nitrogen-doped graphene synthesized via a one-pot hydrothermal process towards oxygen reduction reaction. *J. Power Sources* **2013**, *227*, 185–190.
94. Park, M.; Lee, T.; Kim, B.-S. Covalent functionalization based heteroatom doped graphene nanosheet as a metal-free electrocatalyst for oxygen reduction reaction. *Nanoscale* **2013**, *5*, 12255–12260.
95. Yasuda, S.; Yu, L.; Kim, J.; Murakoshi, K. Selective nitrogen doping in graphene for oxygen reduction reactions. *Chem. Commun.* **2013**, *49*, 9627–9629.
96. Xing, T.; Zheng, Y.; Li, L.H.; Cowie, B.C.C.; Gunzelmann, D.; Qiao, S.Z.; Huang, S.M.; Chen, Y. Observation of active sites for oxygen reduction reaction on nitrogen-doped multilayer graphene. *ACS Nano* **2014**, *8*, 6856–6862.
97. Lai, L.; Potts, J.R.; Zhan, D.; Wang, L.; Poh, C.K.; Tang, C.; Gong, H.; Shen, Z.; Lin, J.; Ruoff, R.S. Exploration of the active center structure of nitrogen-doped graphene-based catalysts for oxygen reduction reaction. *Energy Environ. Sci.* **2012**, *5*, 7936–7942.
98. Yang, S.; Zhi, L.; Tang, K.; Feng, X.; Maier, J.; Muellen, K. Efficient synthesis of heteroatom (N or S)-doped graphene based on ultrathin graphene oxide-porous silica sheets for oxygen reduction reactions. *Adv. Funct. Mater.* **2012**, *22*, 3634–3640.
99. Jiang, Z.J.; Jiang, Z.Q.; Chen, W.H. The role of holes in improving the performance of nitrogen-doped holey graphene as an active electrode material for supercapacitor and oxygen reduction reaction. *J. Power Sources* **2014**, *251*, 55–65.
100. Yu, D.S.; Wei, L.; Jiang, W.C.; Wang, H.; Sun, B.; Zhang, Q.; Goh, K.L.; Si, R.M.; Chen, Y. Nitrogen doped holey graphene as an efficient metal-free multifunctional electrochemical catalyst for hydrazine oxidation and oxygen reduction. *Nanoscale* **2013**, *5*, 3457–3464.
101. Lin, Z.Y.; Song, M.K.; Ding, Y.; Liu, Y.; Liu, M.L.; Wong, C.P. Facile preparation of nitrogen-doped graphene as a metal-free catalyst for oxygen reduction reaction. *Phys. Chem. Chem. Phys.* **2012**, *14*, 3381–3387.

102. Lin, Z.Y.; Waller, G.; Liu, Y.; Liu, M.L.; Wong, C.P. Facile synthesis of nitrogen-doped graphene via pyrolysis of graphene oxide and urea, and its electrocatalytic activity toward the oxygen-reduction reaction. *Adv. Energy Mater.* **2012**, *2*, 884–888.
103. Unni, S.M.; Devulapally, S.; Karjule, N.; Kurungot, S. Graphene enriched with pyrrolic coordination of the doped nitrogen as an efficient metal-free electrocatalyst for oxygen reduction. *J. Mater. Chem.* **2012**, *22*, 23506–23513.
104. Zhang, Y.J.; Fugane, K.; Mori, T.; Niu, L.; Ye, J.H. Wet chemical synthesis of nitrogen-doped graphene towards oxygen reduction electrocatalysts without high-temperateure pyrolysis. *J. Mater. Chem.* **2012**, *22*, 6575–6580.
105. Lin, Z.Y.; Waller, G.H.; Liu, Y.; Liu, M.L.; Wong, C.P. Simple preparation of nanoporous few-layer nitrogen-doped graphene for use as an efficient electrocatalyst for oxygen reduction and oxygen evolution reactions. *Carbon* **2013**, *53*, 130–136.
106. Lu, Z.J.; Bao, S.J.; Gou, Y.T.; Cai, C.J.; Ji, C.C.; Xu, M.W.; Song, J.; Wang, R.Y. Nitrogen-doped reduced-graphene oxide as an efficient metal-free electrocatalyst for oxygen reduction in fuel cells. *RSC Adv.* **2013**, *3*, 3990–3995.
107. Pan, F.P.; Jin, J.T.; Fu, X.G.; Liu, Q.; Zhang, J.Y. Advanced oxygen reduction electrocatalyst based on nitrogen-doped graphene derived from edible sugar and urea. *ACS Appl. Mater. Interfaces* **2013**, *5*, 11108–11114.
108. Zheng, B.; Wang, J.; Wang, F.B.; Xia, X.H. Synthesis of nitrogen doped graphene with high electrocatalytic activity toward oxygen reduction reaction. *Electrochem. Commun.* **2013**, *28*, 24–26.
109. Cong, H.P.; Wang, P.; Gong, M.; Yu, S.H. Facile synthesis of mesoporous nitrogen-doped graphene: An efficient methanol-tolerant cathodic catalyst for oxygen reduction reaction. *Nano Energy* **2014**, *3*, 55–63.
110. Vikkisk, M.; Kruusenberg, I.; Joost, U.; Shulga, E.; Kink, I.; Tammeveski, K. Electrocatalytic oxygen reduction on nitrogen-doped graphene in alkaline media. *Appl. Catal. B* **2014**, *147*, 369–376.
111. Liu, M.K.; Song, Y.F.; He, S.X.; Tjiu, W.W.; Pan, J.S.; Xia, Y.Y.; Liu, T.X. Nitrogen-doped graphene nanoribbons as efficient metal-free electrocatalysts for oxygen reduction. *ACS Appl. Mater. Interfaces* **2014**, *6*, 4214–4222.
112. Ouyang, W.; Zeng, D.; Yu, X.; Xie, F.; Zhang, W.; Chen, J.; Yan, J.; Xie, F.; Wang, L.; Meng, H.; *et al.* Exploring the active sites of nitrogen-doped graphene as catalysts for the oxygen reduction reaction. *Int. J. Hydrogen Energy* **2014**, *39*, 15996–16005.
113. Wang, Z.; Li, B.; Xin, Y.; Liu, J.; Yao, Y.; Zou, Z. Rapid synthesis of nitrogen-doped graphene by microwave heating for oxygen reduction reactions in alkaline electrolyte. *Chin. J. Catal.* **2014**, *35*, 509–513.
114. Chen, L.; Du, R.; Zhu, J.; Mao, Y.; Xue, C.; Zhang, N.; Hou, Y.; Zhang, J.; Yi, T. Three-dimensional nitrogen-doped graphene nanoribbons aerogel as a highly efficient catalyst for the oxygen reduction reaction. *Small* **2015**, *11*, 1423–1429.

115. Sun, Z.; Masa, J.; Weide, P.; Fairclough, S.M.; Robertson, A.W.; Ebbinghaus, P.; Warner, J.H.; Tsang, S.C.E.; Muhler, M.; Schuhmann, W. High-quality functionalized few-layer graphene: Facile fabrication and doping with nitrogen as a metal-free catalyst for the oxygen reduction reaction. *J. Mater. Chem. A* **2015**, *3*, 15444–15450.
116. Wu, J.; Ma, L.; Yadav, R.M.; Yang, Y.; Zhang, X.; Vajtai, R.; Lou, J.; Ajayan, P.M. Nitrogen-doped graphene with pyridinic dominance as a highly active and stable electrocatalyst for oxygen reduction. *ACS Appl. Mater. Interfaces* **2015**, *7*, 14763–14769.
117. Zhou, X.; Bai, Z.; Wu, M.; Qiao, J.; Chen, Z. 3-dimensional porous N-doped graphene foam as a non-precious catalyst for the oxygen reduction reaction. *J. Mater. Chem. A* **2015**, *3*, 3343–3350.
118. Kong, X.-K.; Chen, C.-L.; Chen, Q.-W. Doped graphene for metal-free catalysis. *Chem. Soc. Rev.* **2014**, *43*, 2841–2857.
119. Yu, L.; Pan, X.; Cao, X.; Hu, P.; Bao, X. Oxygen reduction reaction mechanism on nitrogen-doped graphene: A density functional theory study. *J. Catal.* **2011**, *282*, 183–190.
120. Zhang, L.; Xia, Z. Mechanisms of oxygen reduction reaction on nitrogen-doped graphene for fuel cells. *J. Phys. Chem. C* **2011**, *115*, 11170–11176.
121. Kim, H.; Lee, K.; Woo, S.I.; Jung, Y. On the mechanism of enhanced oxygen reduction reaction in nitrogen-doped graphene nanoribbons. *Phys. Chem. Chem. Phys.* **2011**, *13*, 17505–17510.
122. Jiao, Y.; Zheng, Y.; Jaroniec, M.; Qiao, S.Z. Origin of the electrocatalytic oxygen reduction activity of graphene-based catalysts: A roadmap to achieve the best performance. *J. Am. Chem. Soc.* **2014**, *136*, 4394–4403.
123. Sun, M.; Liu, H.; Liu, Y.; Qu, J.; Li, J. Graphene-based transition metal oxide nanocomposites for the oxygen reduction reaction. *Nanoscale* **2015**, *7*, 1250–1269.
124. Wang, X.; Sun, G.; Routh, P.; Kim, D.-H.; Huang, W.; Chen, P. Heteroatom-doped graphene materials: Syntheses, properties and applications. *Chem. Soc. Rev.* **2014**, *43*, 7067–7098.
125. Zhou, X.; Qiao, J.; Yang, L.; Zhang, J. A review of graphene-based nanostructural materials for both catalyst supports and metal-free catalysts in pem fuel cell oxygen reduction reactions. *Adv. Energy Mater.* **2014**, *4*.
126. Li, Q.; Pan, H.; Higgins, D.; Cao, R.; Zhang, G.; Lv, H.; Wu, K.; Cho, J.; Wu, G. Metal-organic framework-derived bamboo-like nitrogen-doped graphene tubes as an active matrix for hybrid oxygen-reduction electrocatalysts. *Small* **2015**, *11*, 1443–1452.
127. Yang, G.H.; Li, Y.J.; Rana, R.K.; Zhu, J.J. Pt-Au/nitrogen-doped graphene nanocomposites for enhanced electrochemical activities. *J. Mater. Chem. A* **2013**, *1*, 1754–1762.
128. Imran Jafri, R.; Rajalakshmi, N.; Ramaprabhu, S. Nitrogen doped graphene nanoplatelets as catalyst support for oxygen reduction reaction in proton exchange membrane fuel cell. *J. Mater. Chem.* **2010**, *20*, 7114–7117.
129. Vinayan, B.P.; Nagar, R.; Rajalakshmi, N.; Ramaprabhu, S. Novel platinum–cobalt alloy nanoparticles dispersed on nitrogen-doped graphene as a cathode electrocatalyst for PEMFC applications. *Adv. Funct. Mater.* **2012**, *22*, 3519–3526.
130. Xiong, B.; Zhou, Y.; Zhao, Y.; Wang, J.; Chen, X.; O'Hayre, R.; Shao, Z. The use of nitrogen-doped graphene supporting Pt nanoparticles as a catalyst for methanol electrocatalytic oxidation. *Carbon* **2013**, *52*, 181–192.

131. Chen, P.; Xiao, T.-Y.; Li, H.-H.; Yang, J.-J.; Wang, Z.; Yao, H.-B.; Yu, S.-H. Nitrogen-doped graphene/ZnSe nanocomposites: Hydrothermal synthesis and their enhanced electrochemical and photocatalytic activities. *ACS Nano* **2012**, *6*, 712–719.
132. Parvez, K.; Yang, S.B.; Hernandez, Y.; Winter, A.; Turchanin, A.; Feng, X.L.; Mullen, K. Nitrogen-doped graphene and its iron-based composite as efficient electrocatalysts for oxygen reduction reaction. *ACS Nano* **2012**, *6*, 9541–9550.
133. Bai, J.C.; Zhu, Q.Q.; Lv, Z.X.; Dong, H.Z.; Yu, J.H.; Dong, L.F. Nitrogen-doped graphene as catalysts and catalyst supports for oxygen reduction in both acidic and alkaline solutions. *Int. J. Hydrogen Energy* **2013**, *38*, 1413–1418.
134. Huang, T.; Mao, S.; Pu, H.; Wen, Z.; Huang, X.; Ci, S.; Chen, J. Nitrogen-doped graphene-vanadium carbide hybrids as a high-performance oxygen reduction reaction electrocatalyst support in alkaline media. *J. Mater. Chem. A* **2013**, *1*, 13404–13410.
135. Park, H.W.; Lee, D.U.; Nazar, L.F.; Chen, Z.W. Oxygen reduction reaction using MnO_2 nanotubes/nitrogen-doped exfoliated graphene hybrid catalyst for Li-O_2 battery applications. *J. Electrochem. Soc.* **2013**, *160*, A344-A350.
136. Xiao, J.; Bian, X.; Liao, L.; Zhang, S.; Ji, C.; Liu, B. Nitrogen-doped mesoporous graphene as a synergistic electrocatalyst matrix for high-performance oxygen reduction reaction. *ACS Appl. Mater. Interfaces* **2014**, *6*, 17654–17660.
137. Brownson, D.A.C.; Munro, L.J.; Kampouris, D.K.; Banks, C.E. Electrochemistry of graphene: Not such a beneficial electrode material? *RSC Adv.* **2011**, *1*, 978–988.
138. Choi, C.H.; Chung, M.W.; Kwon, H.C.; Chung, J.H.; Woo, S.I. Nitrogen-doped graphene/carbon nanotube self-assembly for efficient oxygen reduction reaction in acid media. *Appl. Catal. B* **2014**, *144*, 760–766.
139. Li, Y.; Zhou, W.; Wang, H.; Xie, L.; Liang, Y.; Wei, F.; Idrobo, J.-C.; Pennycook, S.J.; Dai, H. An oxygen reduction electrocatalyst based on carbon nanotube-graphene complexes. *Nat. Nanotechnol.* **2012**, *7*, 394–400.
140. Ma, Y.; Sun, L.; Huang, W.; Zhang, L.; Zhao, J.; Fan, Q.; Huang, W. Three-dimensional nitrogen-doped carbon nanotubes/graphene structure used as a metal-free electrocatalyst for the oxygen reduction reaction. *J. Phys. Chem. C* **2011**, *115*, 24592–24597.
141. Ratso, S.; Kruusenberg, I.; Vikkisk, M.; Joost, U.; Shulga, E.; Kink, I.; Kallio, T.; Tammeveski, K. Highly active nitrogen-doped few-layer graphene/carbon nanotube composite electrocatalyst for oxygen reduction reaction in alkaline media. *Carbon* **2014**, *73*, 361–370.
142. Liu, J.Y.; Wang, Z.; Chen, J.Y.; Wang, X. Nitrogen-doped carbon nanotubes and graphene nanohybrid for oxygen reduction reaction in acidic, alkaline and neutral solutions. *J. Nano Res.* **2015**, *30*, 50–58.